

## RESEARCH ARTICLE

10.1002/2016GB005483

## Key Points:

- A simple mechanistic model of riverine plume behavior on the continental shelf is developed
- The model is used to estimate residence times of plume water on continental shelves globally
- The residence times are used to estimate the amounts of riverine nitrogen and phosphorus that cross the shelf and reach the open ocean

## Supporting Information:

- Data Set S1
- Data Set S2

## Correspondence to:

J. Sharples,  
jonathan.sharples@liverpool.ac.uk

## Citation:

Sharples, J., J. J. Middelburg, K. Fennel, and T. D. Jickells (2016), What proportion of riverine nutrients reaches the open ocean?, *Global Biogeochem. Cycles*, 31, doi:10.1002/2016GB005483.

Received 15 JUL 2016

Accepted 5 DEC 2016

Accepted article online 9 DEC 2016

©2016. The Authors.

This is an open access article under the terms of the Creative Commons Attribution License, which permits use, distribution and reproduction in any medium, provided the original work is properly cited.

## What proportion of riverine nutrients reaches the open ocean?

Jonathan Sharples<sup>1</sup> , Jack J. Middelburg<sup>2</sup> , Katja Fennel<sup>3</sup> , and Timothy D. Jickells<sup>4</sup> 

<sup>1</sup>School of Environmental Sciences, University of Liverpool, Liverpool, UK, <sup>2</sup>Department of Earth Sciences, Utrecht University, Utrecht, Netherlands, <sup>3</sup>Department of Oceanography, Dalhousie University, Halifax, Nova Scotia, Canada, <sup>4</sup>School of Environmental Sciences, University of East Anglia, Norwich, UK

**Abstract** Globally, rivers deliver significant quantities of nitrogen (N) and phosphorus (P) to the coastal ocean each year. Currently, there are no viable estimates of how much of this N and P escapes biogeochemical processing on the shelf to be exported to the open ocean; most models of N and P cycling assume that either all or none of the riverine nutrients reach the open ocean. We address this problem by using a simple mechanistic model of how a low-salinity plume behaves outside an estuary mouth. The model results in a global map of riverine water residence times on the shelf, typically a few weeks at low latitudes and up to a year at higher latitudes, which agrees well with observations. We combine the map of plume residence times on the shelf with empirical relationships that link residence time to the proportions of dissolved inorganic N (DIN) and P (DIP) exported and use a database of riverine nutrient loads to estimate the global distribution of riverine DIN and DIP supplied to the open ocean. We estimate that 75% of DIN and 80% of DIP reaches the open ocean. Ignoring processing within estuaries yields annual totals of 17 Tg DIN and 1.2 Tg DIP reaching the open ocean. For DIN this supply is about 50% of that supplied via atmospheric deposition, with significant east-west contrasts across the main ocean basins. The main sources of uncertainty are exchange rates across the shelf break and the empirical relationships between nutrient processing and plume residence time.

### 1. Introduction

Rivers are the primary conduit transporting weathered, leached, and human-derived material from land to the sea. Rivers deliver 300–380 Tg of organic carbon per year to the coastal zone [Seitzinger *et al.*, 2010], along with important quantities of nitrogen (37–66 Tg total nitrogen  $\text{yr}^{-1}$ ), phosphorus (4–11 Tg total phosphorus  $\text{yr}^{-1}$ ) [Seitzinger *et al.*, 2005; Mayorga *et al.*, 2010; Beusen *et al.*, 2016], and silicate (340–380 Tg DSi  $\text{yr}^{-1}$ ) [Treguer *et al.*, 1995; Beusen *et al.*, 2009; Frings *et al.*, 2016], which contribute significantly to material balances of the ocean. Anthropogenic pressures, particularly wastewater discharge and agricultural activity, are driving significant increases in riverine nutrient loads. The riverine source of reactive N is now about twice the pre-industrial supply, and P has increased by about a factor 3 [Seitzinger *et al.*, 2010]. Sediment retention behind dams is expected to reduce riverine supplies of nitrogen [Harrison *et al.*, 2012], phosphorus [Maavara *et al.*, 2015], and silicate [Laruelle *et al.*, 2009].

Shelf sea ecosystems are affected by these fluvial inputs and in turn modify the biogeochemistry of the open ocean by retaining, exchanging, or breaking down nutrients and organic carbon. Our understanding and ability to predict global biogeochemical cycles currently lacks a realistic treatment of the role of shelf seas in modifying land-derived nutrient and carbon inputs to the open ocean. River point sources and their adjacent shelf systems are poorly represented, if at all, in global biogeochemical models due to insufficient spatial and process resolution. Some budgets of oceanic nutrients assume that all riverine nutrients are retained on the shelf [Duce *et al.*, 2008; Moore and Doney, 2007]. At the other extreme budgets include riverine inputs with no or limited consideration of processing on the shelf [Bernard *et al.*, 2011; Giraud *et al.*, 2008]. There are global box models accounting for nutrient processing at the land-ocean interface, but these have no or very limited geographic resolution [Laruelle *et al.*, 2009; Rabouille *et al.*, 2001]. To some extent, these differences represent boundary definition issues over whether the coastal oceans are included within the ocean or described separately. However, given the very different physical and biogeochemical environments on the shelf and in the deep ocean and the different societal pressures on these systems, it is appropriate to consider the shelf and open ocean separately. Shelf sea biogeochemical processes demand much more nutrients than can be supplied by rivers, with the exchange of shelf water with the open ocean involving a supply of deep ocean

material onto the shelf [e.g., *Fennel et al.*, 2006]. Thus, a more complete picture of global nutrient cycling needs to quantify both how processes on the continental shelves modify riverine material prior to entry into the open ocean and how the shelf system receives and transforms material supplied from the ocean. Improved global models of coastal ocean carbon cycling have begun to be developed [*MacKenzie et al.*, 2000; *Regnier et al.*, 2013; *Bourgeois et al.*, 2016], but to date, less attention has been focused on nitrogen and phosphorus.

A more accurate picture of the effects of riverine nutrients and organic carbon on global ocean biogeochemical cycling requires an informed understanding of how the efficiency of riverine delivery via the continental shelf to the open ocean varies geographically. Riverine inputs can be modified significantly within estuaries and the coastal zone. In the case of phosphorus particle-water exchanges can either enhance or reduce the flux of dissolved phosphorus into coastal waters [*Prastka et al.*, 1998]. In the case of nitrogen, particularly nitrate, any estuarine and coastal processes are likely to involve denitrification and hence could systematically lower riverine inputs. For dissolved organic carbon (DOC), estuaries and coastal waters can be sources or sinks depending on the roles of phytoplankton production and microbial degradation. These processes depend on several factors, including the suspended solids regime, the dissolved and particulate nutrient concentrations, and processes that reflect catchment and estuarine geography [*Statham*, 2012]. Our focus here is on the role of biogeochemical processing in coastal waters outside estuaries, on the continental shelf, in determining the proportion of riverine dissolved inorganic nitrogen (DIN) and dissolved inorganic phosphorus (DIP) that reaches the open ocean. Our approach does not include estuarine processing of N and P, which is a more difficult problem to address on a global scale. It has been suggested that 30–65% of N and 10–55% of P is removed inside estuaries before the material reaches the shelf [*Nixon et al.*, 1996]. More recently, *Jickells and Weston* [2011] have pointed out that estuaries with short residence times will have less effect on the amount of material reaching the shelf.

In this paper we use the residence time of riverine plume water in shelf systems as a useful determinant of the fractions of dissolved N and P that are processed on the shelf before they can reach the open ocean [*Nixon et al.*, 1996; *Seitzinger et al.*, 2006]. We estimate DIN and DIP delivery to the open ocean based on the NEWS 2 database of riverine nutrient loads [*Mayorga et al.*, 2010]. The physical processes that determine residence times of riverine water on the shelf vary considerably, and with over 6000 rivers in the NEWS database it is impractical to attempt any detailed assessment of the physical oceanography around each river input to the shelf. Even limiting such an analysis to the set of rivers responsible for, say, 80% of global N and P delivery to the continental shelves would entail knowing the physical conditions associated with about 440 (for N) and 300 (for P) river mouths. Instead, we develop a mechanistic description of plume behavior that uses simple physical parameters combined with observational estimates of their global variability. This yields an answer, with an envelope of uncertainty, to the riverine nutrient delivery problem that substantially improves on the “all” or “none” approaches currently used when modeling the global impacts of riverine nutrient supplies. While we focus on riverine supplies of N and P, our approach is also relevant to other nutrients and organic carbon and to assessing past and future changes in riverine supplies.

Our method is rooted in the basic physical dynamics of how low-salinity estuarine flows behave on the shelf and how plume or shelf water is exchanged with the open ocean. To make the problem solvable on a global scale, we make approximations about the physics of plume behavior and shelf-ocean exchange. We highlight the areas of uncertainty in these approximations but also demonstrate the robustness of our results. We make estimates of both the proportions of nutrients reaching the open ocean and their absolute magnitudes, though without estuarine processing, the latter should be viewed as upper limits, at least for nitrogen. Our results indicate significant and systematic regional variability in where rivers are able to supply materials to the open ocean, with important implications for the use of current global riverine nutrient load estimates. The results provide a method for inclusion of riverine nutrient supplies in global models that are more realistic than simply assuming that either all or none of the riverine dissolved N and P load reaches the open ocean.

## 2. Methods

The amount of riverine nutrients transported past the shelf break and into the open ocean will depend on the time available for biogeochemical processing of the nutrients on the shelf [*Nixon et al.*, 1996; *Seitzinger et al.*, 2006]. This residence time of riverine water on the shelf is dependent on the physical characteristics of low-salinity plumes on the shelf and by the shelf width (varying from a few tens of kilometers on geologically

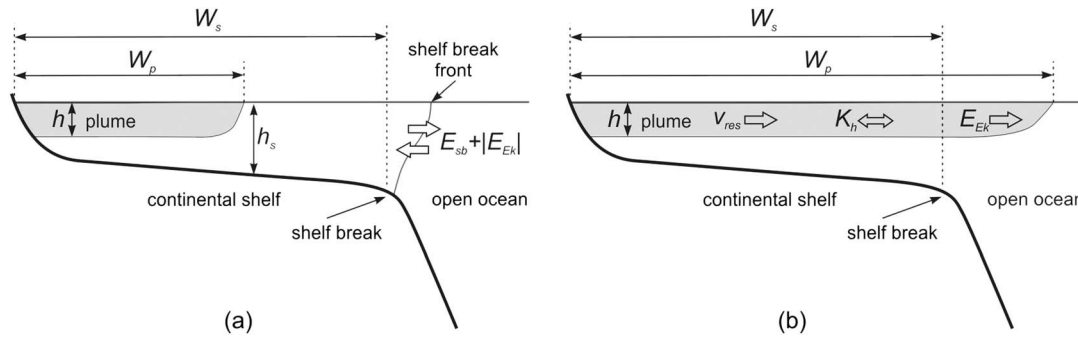


**Figure 1.** Schematic diagram of the physical framework used to assess plume residence times on the shelf. (a) For a plume with width  $W_p$  less than the shelf width  $W_s$  plume water is assumed to be relatively efficiently mixed into the shelf water. Exchange with the open ocean is limited by the generally weak exchange processes at the shelf break, taken as a combination of wind-driven Ekman transport ( $E_{EK}$ ) and other shelf break processes ( $E_{sb}$ ). (b) For a plume that extends beyond the shelf break, transport of plume water over the shelf break is taken to be a combination of residual cross-plume flow ( $v_{res}$ ), horizontal dispersion through the plume ( $K_h$ ), and wind-driven Ekman exchange driving surface water off the shelf.

active coasts associated with subduction zones to several hundreds of kilometers in geologically passive regions). We first develop a simple mechanistic model of how a plume operates outside the mouth of an estuary. This leads to a global picture of the average time riverine material spends on the shelf before it is transferred to the open ocean, along with uncertainty estimates of this residence time. We use this knowledge of residence time, along with empirical relations linking residence time to the proportion of dissolved inorganic N and P that can be processed in aquatic systems, to yield a global map of the proportions of riverine N and P that reach the open ocean.

### 2.1. A Mechanistic Model of Low-Salinity Plumes and Exchange With the Open Ocean

A low-salinity plume of water exiting an estuary and entering the shelf sea will be diverted by the Earth's rotation against the coast to form a buoyancy-driven current. Our method is based on using the cross-shelf width of this buoyancy current compared to the width of the local continental shelf as a determinant of what processes transport riverine material across the shelf break and into the open ocean. The concept, along with important parameters and definitions, is summarized in the schematic diagram in Figure 1.

The width of a coastal buoyancy current is related to the internal Rossby radius [Narayanan and Garvine, 2002; Yankovsky and Chapman, 1997]. Assuming that the buoyancy current flows as a two-layer, stratified system, the internal Rossby radius is

$$R'_0 = \frac{c}{f} \tag{1}$$

The Coriolis frequency  $f = 2\omega \sin\phi$  ( $s^{-1}$ ), with  $\omega$  the rotational frequency of the Earth and  $\phi$  latitude, and the internal wave speed,  $c$ , is given by

$$c = \sqrt{g'h} \tag{2}$$

with  $h$  (m) the thickness of the surface layer. The reduced gravity  $g' = g \frac{\Delta\rho}{\rho_0}$  with  $g$  gravitational acceleration ( $9.81 \text{ m s}^{-2}$ ),  $\rho_0$  ( $\text{kg m}^{-3}$ ) the typical shelf water density, and  $\Delta\rho$  the density contrast between the surface plume and underlying shelf water ( $\text{kg m}^{-3}$ ). The internal Rossby radius is thus dependent on latitude, as well as on the local stratification and the vertical extent of the low-salinity plume. At each river mouth we consider the following question: is the width of the coastal buoyancy current less than or greater than the width of the shelf? If the buoyancy current extends beyond the shelf break, then we assume that the residence time of plume water over the shelf is governed by the cross-plume residual flows, wind-driven Ekman transport, and horizontal dispersion within the buoyancy current. If the buoyancy current is narrower than the shelf, then we assume that the exchange of plume water with the shelf water is far more effective than the exchange of shelf water across the shelf break. This often results in a shelf break front, separating water with lower salinity on the shelf from the open ocean [e.g., Brink, 1998]. Exchange between the shelf and the open ocean is constrained by the generally weak shelf break processes [e.g., Huthnance, 1995].

We assume that the width of the coastal buoyancy current,  $W_p$ , is related to the internal Rossby radius by  $W_p = aR'_0$ . Calculating an accurate value of  $R'_0$  and  $a$  for all rivers in the NEWS database is not possible, so

**Table 1.** Parameters Used in the Analysis to Yield Values of  $a = \frac{W_p}{R'_o}$

Parameter	Description	Units	Source
$\Delta\rho$	Density difference between plume water and underlying shelf water	$\text{kg m}^{-3}$	Observations (Table 2)
$h$	Vertical extent of the plume surface layer	m	Observations (Table 2)
$\varphi$	Latitude	degree	Observations (Table 2)
$f$	Coriolis parameter	$\text{s}^{-1}$	Calculated (see text)
$c$	Internal wave speed	$\text{m s}^{-1}$	Calculated (equation (2))
$R'_o$	Internal Rossby radius	m	Calculated (equation (1))
$W_p$	Width of a low-salinity plume	m	Observations (Table 2)
$a$	Scaling factor relating plume width to the internal Rossby radius	none	Calculated, $a = \frac{W_p}{R'_o}$

instead, we aim to use observations of plumes to provide useful global mean values of  $c$  (equation (2)) and  $a$ . We also quantify the variability in  $c$  and  $a$  which are used to yield uncertainty estimates for our calculations of DIN and DIP export to the open ocean. Table 1 summarizes the parameters required in our analysis.

This assumption that the buoyancy current width scales with  $R'_o$  is a key simplification. We will first consider aspects of plume physics that numerical experiments have shown to have the potential for undermining this scaling and then draw on observations of river plume widths to demonstrate that the assumption is valid with some quantifiable uncertainty.

### 2.1.1. Other Influences on Plume Width

There are aspects of plume physics that can increase the cross-shelf extent of the buoyancy discharge beyond the constraints imposed via  $R'_o$  [e.g., *Horner-Devine et al.*, 2015]. If these aspects are common and have a significant effect, they could undermine our method in that a plume that we consider constrained to the shelf could reach beyond the shelf break. We will consider four such aspects: an initial anticyclonic bulge in the low-salinity discharge prior to development of the buoyancy current [*Nof and Pichevin*, 2001], strong inflow speeds combined with weak stratification at the mouth of the discharge [*Yankovsky and Chapman*, 1997], plumes that are attached to the seabed rather than confined to a buoyant surface layer [*Yankovsky and Chapman*, 1997], and river mouths that are wide compared to  $R'_o$  [*Narayanan and Garvine*, 2002].

First, theoretical analysis suggests that the alongshore momentum flux in a steady coastal buoyancy current needs to be balanced by the development of a low-salinity bulge with an anticyclonic rotation at the river mouth [*Nof and Pichevin*, 2001]. For the majority of river mouths most of the river discharge then joins the coastal buoyancy current, with a circulation time scale around the initial bulge of about an inertial period ( $\sim 1/f$ ). Numerical experiments of river discharges at the coast often show such features, with the offshore extent of the bulge potentially reaching several times farther than the width of the downstream coastal buoyancy current [*Fong and Geyer*, 2002]. However, observations of coastal plumes rarely show a bulge [e.g., *Garvine*, 2001] (but see *Horner-Devine et al.* [2009] for an example of an observed bulge) with discharge turning to the right (Northern Hemisphere) to form the coastal buoyancy current scaled by  $R'_o$ . The occurrence of the initial bulge in numerical and laboratory experiments has been ascribed to the lack of ambient coastal flows or surface winds in models [*Fong and Geyer*, 2002; *Horner-Devine et al.*, 2015] and also to the simplified coastal and river mouth geometries used in the model experiments [*Garvine*, 2001]. In cases where a bulge does occur, the circulation time scale within the bulge is short compared to the processing time scales of DIN and DIP, and so we still expect the relevant residence time of riverine DIN and DIP to be determined by the post-bulge buoyancy current.

Next we consider the effect of a strong river flow, with flow out of the river mouth of  $v$  and the reduced gravity in the plume given by  $g' = g^{\Delta\rho}/\rho_0$ . If

$$v^2 \gg g'h, \quad (3)$$

i.e.,  $v \gg c$ , then the plume extent offshore becomes governed by  $v/f$  rather than by  $R'_o = c/f$  [*Yankovsky and Chapman*, 1997]. The outflow current at the river mouth can be estimated by applying a steady state salt balance (the Knudsen relation [*Knudsen*, 1900]) with the river discharge,  $Q$  ( $\text{m}^3 \text{s}^{-1}$ ), through the mouth cross-sectional area,  $A$  ( $\text{m}^2$ ). The flow out of the river is then

$$v = \frac{s_0 Q}{\Delta s A} \quad (4)$$

**Table 2.** Plume Parameters for a Range of Low-Salinity Plumes<sup>a</sup>

River	$Q$ ( $\times 10^3 \text{ m}^3 \text{ s}^{-1}$ )	$\Delta\rho$ ( $\text{kg m}^{-3}$ )	$h$ (m)	$\phi$ (deg)	$W_p$ (km)	$c$ ( $\text{m s}^{-1}$ )	$R'_o$ (km)	$a$	$S_p$
Amazon <sup>b</sup>	204	7	10	2	250	0.81	81	3.1	2.0
Sepik <sup>c</sup>	7	24	1.5	4	75	0.59	59	1.3	3.0
Congo/Nyanga <sup>d</sup>	40	7.5	1.5	6	110	0.32	21	5.2	2.5
Zambezi <sup>e</sup>	3.4	3.3	8	18	35	0.5	11	3.2	0.8
Pearl (high) <sup>f</sup>	8.7	20	5	22	70	0.98	18	3.9	0.5
Pearl (low) <sup>f</sup>	2.9	3.3	3	22	20	0.31	5.7	3.5	0.1
Tsengwen <sup>g</sup>	0.06	0.8	2	23	2.3	0.12	2.2	1	0.1
Mississippi <sup>h</sup>	16.8	5	5	29	50	0.5	7	7.1	0.8
Mekong (high) <sup>i</sup>	39	8	5	34	45	0.61	7.6	5.9	0.2
Mekong (low) <sup>i</sup>	16	8	2	34	25	0.39	4.8	5.2	0.1
Chesapeake Bay <sup>j</sup>	2.2	3.3	5	37	10	0.4	4.5	2.2	0.04
Delaware <sup>k</sup>	0.31	5	7	39	20	0.58	7	2.9	0.15
Llobregat <sup>l</sup>	0.05	1.6	2	41	5.6	0.18	1.8	3.1	0.4
Rhone <sup>m</sup>	2	3.3	7	43	25	0.47	4.8	5.2	0.8
Danube <sup>n</sup>	6.3	7	8	44.5	20	0.73	7.2	2.8	0.3
Columbia <sup>o</sup>	7.6	3	10	46	40	0.53	5.1	7.8	1.0
Rhine <sup>p</sup>	2.3	2	5	52	20	0.3	2.7	7.4	0.03
Mersey <sup>q</sup>	0.13	1.5	10	53	15	0.38	3.3	4.5	0.02
MacKenzie <sup>r</sup>	10	8	6	69	25	0.68	5	5	0.2
Yenisei/Ob <sup>s</sup>	32	13	15	73	50	1.4	10	5	0.01

<sup>a</sup>Most parameters are taken from studies that present sufficient observational data or well-verified model data to determine stratification and plume width, allowing  $c$ ,  $R'_o$ ,  $a$ , and  $S_p$  to be calculated.

<sup>b</sup>Geyer *et al.* [1996].

<sup>c</sup>Higgins *et al.* [2006].

<sup>d</sup>Denamiel *et al.* [2013].

<sup>e</sup>Nehama and Reason [2014].

<sup>f</sup>Dong *et al.* [2004].

<sup>g</sup>Liu *et al.* [1999].

<sup>h</sup>Rabalais *et al.* [2002] and Schiller *et al.* [2011].

<sup>i</sup>Hordoir *et al.* [2006].

<sup>j</sup>Rennie *et al.* [1999].

<sup>k</sup>Whitney and Garvine [2006].

<sup>l</sup>Liste *et al.* [2014].

<sup>m</sup>Estournel *et al.* [2001].

<sup>n</sup>Moebius and Daehnke [2015].

<sup>o</sup>Hickey *et al.* [2005].

<sup>p</sup>Simpson *et al.* [1993].

<sup>q</sup>Polton *et al.* [2011] and Sharples and Simpson [1993].

<sup>r</sup>Mulligan *et al.* [2010].

<sup>s</sup>Zatsepin *et al.* [2010].

with  $s_0$  the bottom water salinity and  $\Delta s$  the salinity stratification. We can illustrate this with estimates of  $v$  and  $c$  for a range of river discharges. The river Rhine is an example of a low discharge, temperate river (Table 2). The Rhine has a mean river discharge of  $2000 \text{ m}^3 \text{ s}^{-1}$ , about 60% of which flows through the Nieuwe Waterweg with a width 2 km and mean depth 15 m. With  $\Delta s \sim 2.5$  and  $s_0 \sim 32$  [Simpson *et al.*, 1993] equation (4) suggests a mean  $v \approx 0.5 \text{ m s}^{-1}$ , which compares to  $c \sim 0.3 \text{ m s}^{-1}$  (Table 2). An example toward the other extreme of freshwater discharge is the Mekong during the wet season (Table 2), a low-latitude river with a discharge of  $35,000 \text{ m}^3 \text{ s}^{-1}$  through a mouth of width about 30 km and  $h \approx 5 \text{ m}$  [Hordoir *et al.*, 2006]. Using  $\Delta s \sim 12$  and  $s_0 \sim 20$  just outside the estuary mouth [Hordoir *et al.*, 2006], equation (4) suggests  $v \approx 0.4 \text{ m s}^{-1}$ . The appropriate estimate of  $c$  (Table 2) is  $0.61 \text{ m s}^{-1}$ . Finally, considering an Arctic river in full flood, the MacKenzie River has a peak discharge approaching  $30,000 \text{ m}^3 \text{ s}^{-1}$ , with a mouth of width 10 km, mean depth 10 m,  $\Delta s \sim 10$ , and  $s_0 \sim 32$  [Carmack and MacDonald, 2002]. This yields  $v \sim 1.0 \text{ m s}^{-1}$ , compared to  $c \sim 0.9 \text{ m s}^{-1}$  (Table 2). Thus, even for the case of a high flood discharge, it is unlikely that  $v \gg c$ . These examples are consistent with a general observation that estuarine flows have Froude number,  $v/c$ , less than or equal to 1, and hence, the condition  $v \gg c$  is rarely met.

We now consider the possibility of the buoyant plume remaining attached to the seabed, which could undermine our analyses by widening a narrow buoyancy current so that it reaches beyond the shelf

break. Theoretical analysis [Yankovsky and Chapman, 1997] suggests that a plume originating from a buoyancy source at the coast of width  $L$  and depth  $h_L$  will remain attached to the bed out to a depth of

$$h_b = \left( \frac{2Lv h_L f}{g'} \right)^{1/2} \quad (5)$$

Noting that the cross-section area  $A = Lh_L$  and substituting for  $v$  using equation (4) yields

$$h_b = \left( \frac{2s_0 Q f}{g' \Delta s} \right)^{1/2} \quad (6)$$

Thus, the freshwater discharge required for the plume to remain attached to a depth  $h_b$  is

$$Q = \frac{\Delta s g' h_b^2}{2s_0 f} \quad (7)$$

Based on the data in Table 2, and assuming that the density contrasts are dominated by salinity, the range of  $s_0/\Delta s$  is about 1–30, with an average of about 7, and mean  $g' = 0.06 \text{ m s}^{-2}$ . For a midlatitude plume ( $f \sim 5 \times 10^{-5} \text{ s}^{-1}$ ) to remain attached to the seabed out to a depth of  $h_b = 50 \text{ m}$ , equation (7) suggests that the discharge  $Q$  needs to be  $\sim 2 \times 10^5 \text{ m}^3 \text{ s}^{-1}$ , i.e., similar to the Amazon discharge. While strong discharges from a river mouth may be able to keep the plume attached to the seabed and so reach farther offshore than we might predict using the simple scaling with  $R'_o$ , it is not feasible for the plume to remain attached out to the continental shelf edge (depths typically  $> 50 \text{ m}$ ). Hence, if our internal Rossby radius consideration predicts that a plume is confined to the shelf, including potential bottom attachment cannot switch the plume to one that reaches beyond the shelf edge.

Finally, river discharge with a mouth wider than the internal Rossby radius can drive a plume to several times  $R'_o$  [Narayanan and Garvine, 2002]. In our analyses the most likely region for this to occur is over the relatively narrow shelf of the Canadian Arctic, where the high latitude results in a small internal Rossby radius of 3–5 km and our analyses would suggest that riverine water is confined to a plume on the shelf. The mouth of the MacKenzie River has a width of about  $4R'_o$ , with theoretical analyses [Narayanan and Garvine, 2002] suggesting that the plume can reach 5 times  $R'_o$ . The shelf width here is typically 50–150 km, so that despite the increased plume width, the river water would still be confined to the shelf.

### 2.1.2. Observed Plume Widths and the Shelf Width

We now take an empirical approach to estimating a useful scaling of plume parameters and of plume widths based on the local  $R'_o$ . We aim to provide useful global mean values of  $c = \sqrt{g' h}$  and  $a = \frac{W_p}{R'_o}$ . We also quantify the variabilities in  $c$  and  $a$ , which are used to yield uncertainty estimates for our calculations of DIN and DIP export to the open ocean. An analysis was carried out on 20 low-salinity plumes, where sufficient data exist to calculate  $c$  and  $R'_o$  and to assess the observed plume width to quantify a local value of  $a$ , covering a full latitudinal range and including low and high discharge rivers (Table 2). The results give a globally averaged  $c = 0.53$  (0.36–0.63)  $\text{m s}^{-1}$  and plume width described by  $a = 4.3$  (3.1–5.4), where the numbers in brackets are the 95% confidence intervals calculated using a bootstrapping method [Efron and Gong, 1983]. Subsequent analysis for residence times and DIN and DIP export to the ocean will be based on the mean values for  $c$  and plume width; the 95% confidence intervals will be used to provide an assessment of the effect of global variability in plume characteristics on our results. It is perhaps surprising that the range of values for  $c$  is so limited and that there is a viable global mean value for  $c$ . However, once a low-salinity plume has exited onto the shelf, there is a limited parameter space available for  $\Delta\rho$  and  $h$ . While the stratification ranges between about 1 and  $20 \text{ kg m}^{-3}$ , very strong stratification is less common and in the calculation of  $c$  a high  $\Delta\rho$  can be compensated for by low value of  $h$ .

For each river mouth in the NEWS database the shelf edge was identified, based on assessing where the seabed gradient increased marking the top of the continental slope, in the General Bathymetric Chart of the Oceans 08 gridded global bathymetry [General Bathymetric Chart of the Oceans, 2008]. The distance,  $W_s$ , between river mouth and shelf edge was calculated. The estimates of plume width ( $W_p = aR'_o$ ) using

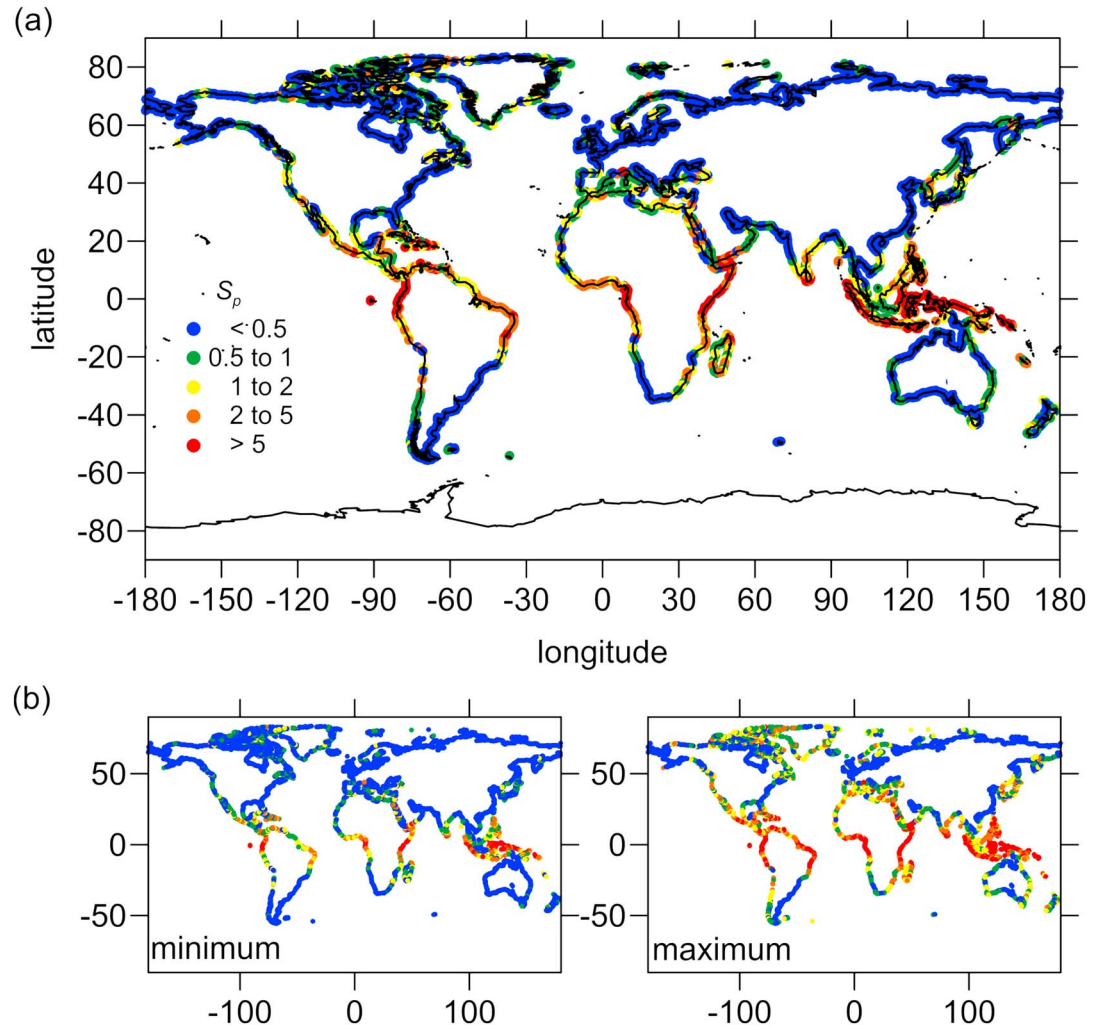


**Figure 2.** (a) Average ratio of plume width to shelf width ( $S_p$ ). (b) Uncertainties in  $S_p$  based on the 95% confidence intervals in  $c$  and  $a$ .

mean values of  $c$  and  $a$ ) were compared to the local shelf width to produce a global map of the ratio of plume width to shelf width:

$$S_p = \frac{W_p}{W_s} \tag{8}$$

(Figure 2a). Values of  $S_p > 1$  are mainly confined to latitudes within  $20^\circ$  of the equator as a result of the strong influence of  $f$  on  $R'_o$ . The effect of narrow shelves can be seen to increase  $S_p$ , for instance, along western North and South America, in the Mediterranean, and in southeast Africa (Figure 2a). Applying the 95% confidence limits to  $c$  and  $a$ , the region of high  $S_p$  not surprisingly tightens in latitudinal range for the lower limits of  $c$  and  $a$ , while at the higher limits areas around the globe with narrow shelf widths shift toward high  $S_p$  (Figure 2b).

### 2.1.3. Estimating Residence Time on the Shelf

The requirement now is for a global map of plume residence time on the continental shelves. We want to quantify the average time it takes water leaving an estuary mouth to cross the shelf break and enter the open ocean. Conceptually, this is similar to calculating the amount of time a river discharge takes to replace the freshwater fraction on the shelf; i.e., the Land-Ocean Interactions in the Coastal Zone method that is primarily useful for well-defined semienclosed shelf regions [Huthnance, 2010]. If  $S_p > 1$ , the low-salinity plume reaches beyond the shelf edge into the open ocean, and the residence time of water over the shelf is assumed to be governed by the cross-shelf transport mechanisms within the buoyant plume. Alternatively, if  $S_p < 1$ , then the low-salinity water will be confined on the shelf within the coastal buoyancy current; plume water will

be gradually stirred into the shelf water and eventual exchange with the open ocean will be controlled by the processes that govern ocean-shelf exchange across the shelf break.

For a wide plume that reaches beyond the shelf break ( $S_p > 1$ ) we consider three processes that can drive plume water offshore:

1. A weak residual cross-plume flow,  $v_{res}$ , is a common feature of low-salinity plumes, ranging from a few centimeters per second in midlatitude plumes [e.g., *Gelfenbaum and Stumpf*, 1993; *Hickey et al.*, 2005; *Narayanan and Garvine*, 2002; *Souza et al.*, 1997] to 20–30  $\text{cm s}^{-1}$  in the Amazon plume [*Geyer et al.*, 1996]. We use minimum and maximum values for  $v_{res}$  of 5 and 25  $\text{cm s}^{-1}$  and calculate a residence time as the transport time between the coast and the shelf edge at speed  $v_{res}$ .
2. Horizontal dispersion will transport material along gradients within the plume, at a rate governed by the horizontal dispersion coefficient,  $K_h$  ( $\text{m}^2 \text{s}^{-1}$ ). Values for  $K_h$  in shelf seas vary between about 100 and 600  $\text{m}^2 \text{s}^{-1}$  [e.g., *Houghton et al.*, 2009; *Sanders and Garvine*, 2001]. Larger values of  $K_h$  are associated with longer experiments where drifters or dye can be affected by large-scale eddy motions. These longer time scales are more appropriate to the problem of plume residence time, so we use  $K_h \sim 500 \text{ m}^2 \text{ s}^{-1}$ . Noting that a dispersive process results in a patch size over a time  $t$  of  $\sim \sqrt{K_h t}$ , we estimate residence time as  $\sim \frac{W_s}{K_h}$ .
3. An efficient mechanism for transporting plume water away from the coast is wind-driven Ekman transport when the wind direction has a component driving coastal upwelling [e.g., *Munchow and Garvine*, 1993]. This process will be strongly regional. We have quantified this globally using the Southampton Oceanography Centre climatology of wind stress forcing [*Josey et al.*, 2002]. For each river mouth the local annual mean wind stress direction was compared to the direction of the shelf break, and the cross-shelf break Ekman transport,  $E_{EK}$  ( $\text{m}^2 \text{s}^{-1}$ ), calculated as

$$E_{EK} = \frac{\tau_{sb}}{\rho_0 f} \quad (9)$$

with  $\tau_{sb}$  ( $\text{N m}^{-2}$ ) the component of wind stress parallel to the shelf break (Figure 3). In areas where the Ekman transport induces upwelling (positive  $E_{EK}$  in Figure 3) a plume transport time scale over the shelf break was calculated as  $\frac{hW_s}{E_{EK}}$ , with the plume depth  $h$  taken as the mean of the plumes in Table 2.

For a plume confined to the shelf ( $S_p < 1$ ), we consider physical processes controlling exchange across the shelf break as the determinant of residence time. These processes vary considerably in different shelf regimes [e.g., *Huthnance*, 1995], and with the exception of wind-driven Ekman exchange, it is difficult to quantify the varying exchange rates globally. We take the following approach:

1. Exchange by wind-driven Ekman transport is quantified for all outflows as in Figure 3. We assume that the longer residence times associated with shelf-constrained plumes result in much of the plume water being dispersed throughout the depth of the shelf sea. Thus, the relevant transport is taken to be the absolute value of the Ekman transport,  $|E_{EK}|$ ; i.e., both upwelling and downwelling transports result in exchange of shelf water containing riverine material with the open ocean, and we assume that there is sufficient contrast in the strength and timing of upwelling and downwelling events to prevent resupply of previously exported water.
2. In addition to wind-driven exchange, there is a variety of other processes that are more difficult to quantify, such as exchange through the Ekman layers of slope currents, internal tides, and eddy and filament exchange. An analysis of these processes along the subtropical and subpolar shelves of the NE Atlantic provides typical values [*Huthnance et al.*, 2009]. Using estimates from 10 shelf regions [*Huthnance et al.*, 2009], we add a mean nonwind-driven exchange contribution of  $E_{sb} = 1.7 \text{ m}^2 \text{ s}^{-1}$  to the local wind-driven Ekman exchange and use the 95% confidence intervals (3.2 and 0.7  $\text{m}^2 \text{ s}^{-1}$ ) to investigate the likely effects of uncertainty in shelf-ocean exchange.

For the shelf-confined plume we estimate residence time as  $\frac{h_s W_s}{(E_{sb} + E_{EK})}$ , with  $h_s$  the mean shelf depth (taken to be half the depth of the local shelf edge).

For both types of plume we first determine an average  $S_p$  for the shelf local to each river in the NEWS database. A mean riverine water residence time on the shelf,  $T_{res}$ , is then calculated based on  $S_p$  and average transport and exchange rates described above appropriate to whether  $S_p$  is greater than or less than 1 (Figure 4a).

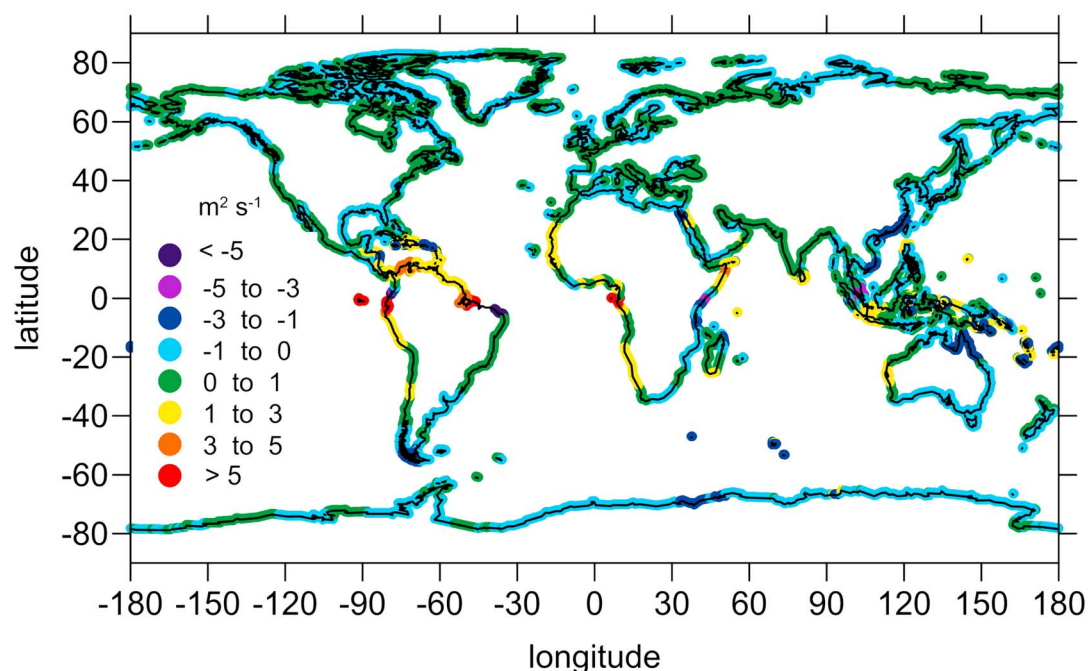


**Figure 3.** Global pattern of annual mean cross-shelf break wind-driven Ekman flux. Off-shelf, or upwelling, fluxes are positive.

Uncertainties in  $T_{res}$  (Figure 4b) use the 95% confidence limits for  $c$  and  $a$  to yield maximum and minimum values for  $S_p$ . A lower limit to  $T_{res}$  uses the maximum  $S_p$  and the fastest transport and exchange rates for the plume type; an upper limit to  $T_{res}$  uses the minimum  $S_p$  and slowest transport and exchange rates. Thus, the lower estimates of  $T_{res}$  arise from wide plumes combined with efficient cross-plume transport or rapid ocean-shelf exchange. The higher estimates of  $T_{res}$  arise from narrow plumes and weak cross-plume transport or ocean-shelf exchange.

The results of our calculation for the residence times compare well with available observations of residence times on a wide range of shelves and over a range of  $T_{res}$  from 1 week to >1 year (Table 3). There is a large range of  $T_{res}$ . The latitudinal distribution of  $T_{res}$  is primarily controlled by the Coriolis parameter,  $f$ , influenced by the distribution of shelf widths causing contrasts in  $T_{res}$  between the eastern and western coasts of North America, South America, and southern Africa. The global variability in Ekman exchange has a smaller effect, localized around strongly upwelling-favorable coasts (Peru, NW Africa, and NE South America). The results indicate that, in general, low-latitude riverine discharges will reach the open ocean quickly (in a few to tens of days). There is also a contrast between Northern and Southern Hemisphere shelves, reflecting the wide shelves found at high northern latitudes. The longest residence times (time scales of a year or more) occur on the wide shelves in middle to high northern latitudes, while narrower midlatitude shelves in the Southern Hemisphere have residence times of 1–3 months. In the Northern Hemisphere the main deviations from this north-south contrast are the shelf of western North America and the shelves around Greenland and the Canadian Arctic, where narrow shelves lead to short residence times. In the Southern Hemisphere the main deviations from the north-south contrast are in southwestern South America and southeastern Africa, where residence times are calculated to be less than 1 month, again as a result of narrow shelves. The uncertainties in these residence times (Figure 4b) can be up to a factor of 2 or 3 away from the mean  $T_{res}$ , though the pattern of very short residence times at low latitudes is consistent.

## 2.2. Residence Time and the Processing of DIN and DIP on the Shelf

Having calculated a global pattern of plume water residence time, along with its uncertainties, and demonstrated that our calculations are consistent with observed residence times, we can now apply this knowledge to the problem of nutrient export from continental shelves. A range of biogeochemical processes affect the rate of turnover of nitrogen and phosphorus in aquatic systems, leading to characteristic time scales of

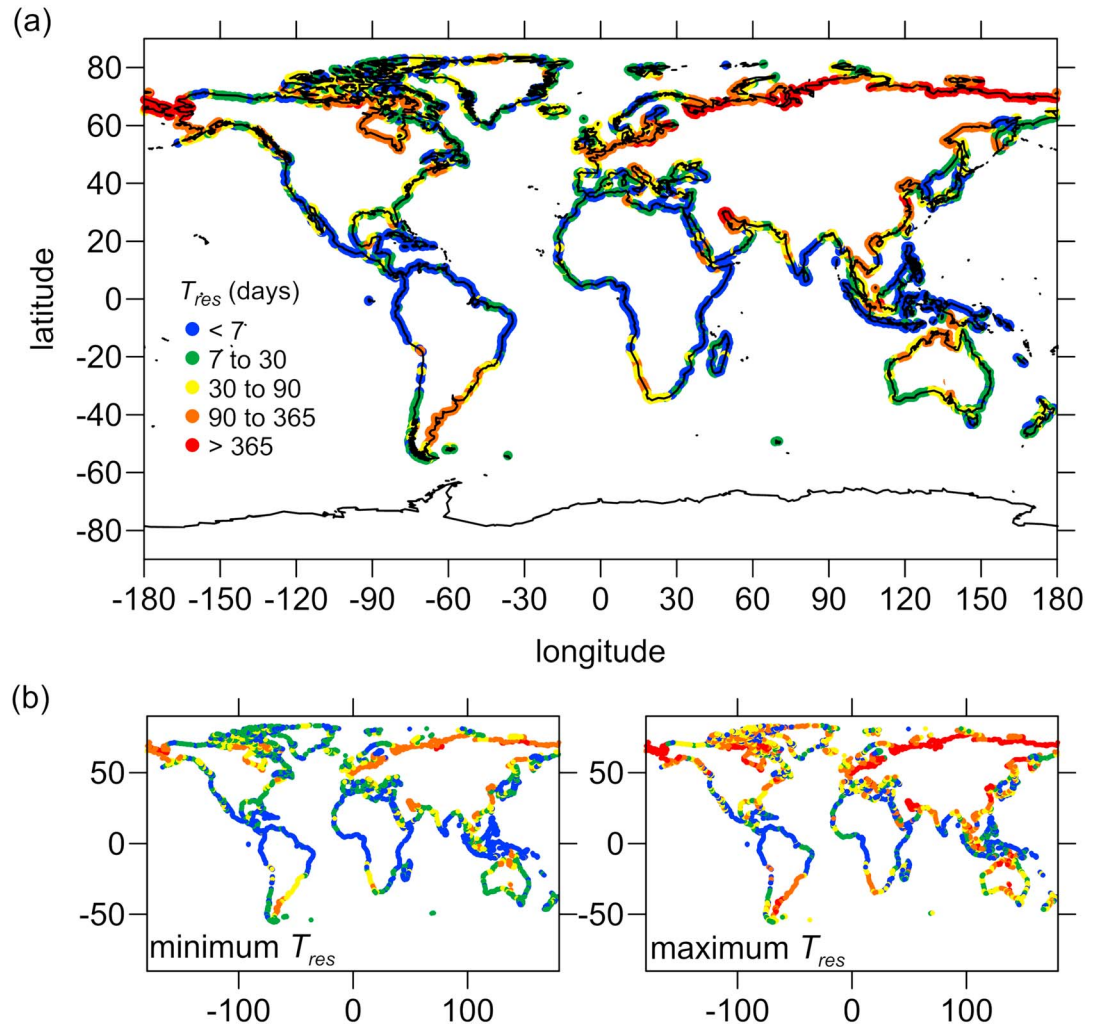


**Figure 4.** (a) Average residence time ( $T_{res}$ ) on the continental shelf. (b) Uncertainties in  $T_{res}$  based on the 95% confidence intervals in  $c$  and plume width and uncertainties in cross-plume and cross-shelf break exchange rates.

biogeochemical process and the cycling of nutrients (dissolved inorganic, dissolved organic, or particulate form) and organic carbon. Phytoplankton and fixed dissolved inorganic nitrogen stocks in midlatitude shelves typically turnover on time scales of  $\sim 1$  week and  $\sim 6$  weeks, respectively [Fennel *et al.*, 2009; Middelburg and Soetaert, 2004], indicating that nutrients are involved in an intensive phytoplankton uptake, deposition, and (sediment) remineralization loop with a time scale of less than 2 months. This nutrient recycling may not provide a permanent sink for P if there is no active depocenter for particulate organic matter within a particular shelf system. However, in the case of nitrogen, part of the nitrogen regenerated in sediments is transformed into dinitrogen gas and lost from the marine system by processes such as denitrification and anaerobic oxidation of ammonium (anammox). These nitrogen gas production rates in continental shelf sediments vary widely but typically are  $\sim 2 \text{ mmol N m}^{-2} \text{ d}^{-1}$  [Fennel *et al.*, 2009; Middelburg and Soetaert, 2004]. Taking a shelf water depth of 50 m and a nitrate concentration of  $10 \mu\text{M}$ , this suggests that it would take  $\sim 250$  days to remove all of the nitrate. So if the residence time of water on the shelf is several months, such as in the middle to high latitudes (Figure 4a), then we would expect that nitrate removal by denitrification and anammox will be effective. Alternatively, in low-latitude regions where we calculate residence times of less than 1 month, we would expect little removal of nitrate before the water is exchanged with the open ocean. We have assumed here, and throughout our analyses, that processing time scales on the shelf are independent of latitude, an approach consistent with the relationships between DIN and DIP removal and residence time [Nixon *et al.*, 1996; Seitzinger *et al.*, 2006].

**Table 3.** Observed Residence Times of Water on Continental Shelves Along With the Estimate Based On the Calculation of  $T_{res}$  (Figure 4a)<sup>a</sup>

Coastal Region	Observed Residence Time	$T_{res}$
North Sea <sup>b</sup>	~1 year	0.4–1 year
Biscay <sup>c</sup>	1–4 months	1–4 months
Iberian shelf <sup>d</sup>	2 weeks	1–6 weeks
New Jersey <sup>e</sup>	1–7 weeks	2–8 weeks
South Atlantic Bight <sup>e</sup>	1–2 months	1 month
Alaska Coastal Current <sup>g</sup>	<~1 year	2 months to 1 year
Monterey Bay <sup>h</sup>	1–2 weeks	1–4 weeks
Chile (38°–40°S) <sup>i</sup>	1 week	1–3 weeks
Brazil (23°S) <sup>j</sup>	1–2 weeks	1 week
East China Sea <sup>k</sup>	1 year	0.5–1 year
Gulf of Carpentaria <sup>l</sup>	~1 year	3 months to 1 year
Great Barrier shelf, Australia <sup>m</sup>	1–4 weeks	2–6 weeks
SW Australia <sup>n</sup>	1–2 weeks	2–4 weeks
Laptev shelf <sup>o</sup>	>1 year	1–2 years

<sup>a</sup>Observed residence times are based on one or more of the following: changes in along-slope water properties, variance in cross-slope flows, or tracks of drifting buoys.

<sup>b</sup>J. M. Huthnance [1997].

<sup>c</sup>J. M. Huthnance et al. [2009].

<sup>d</sup>J. M. Huthnance et al. [2002].

<sup>e</sup>Gong et al. [2010].

<sup>f</sup>W. S. Moore [2007].

<sup>g</sup>Weingartner et al. [2005].

<sup>h</sup>Breaker and Broenkow [1994].

<sup>i</sup>Atkinson et al. [2002].

<sup>j</sup>W. S. Moore and de Oliveira [2008].

<sup>k</sup>Ren et al. [2006].

<sup>l</sup>Condie [2011].

<sup>m</sup>Choukroun et al. [2010].

<sup>n</sup>Gersbach et al. [1999].

<sup>o</sup>Eicken et al. [2005].

Empirical relationships for the removal of DIN within a system [Seitzinger et al., 2006] and the export of DIP from a system [Nixon et al., 1996] are reproduced in Figure 5. Quantifying the empirical relation for DIN (Figure 5a) suggests that the proportion of DIN removed by biogeochemical processes from an aquatic system,  $N_{rem}$ , is related to residence time  $T_{res}$  (months) by

$$N_{rem} = 23.9T_{res}^{0.2} \% \quad (10)$$

with an uncertainty, based on the root-mean-square deviation about the fitted curve, of  $\pm 15\%$ . For the proportion of DIP exported from a system,  $P_{ex}$ , the fit in Figure 5b provides

$$P_{export} = 80.5 - 13.8 \ln T_{res} \% \quad (11)$$

with an uncertainty of  $\pm 14\%$ . To make the DIN and DIP equations consistent, we also deal in the percentage of DIN exported from a system and so write

$$N_{export} = 100 - N_{rem} \% \quad (12)$$

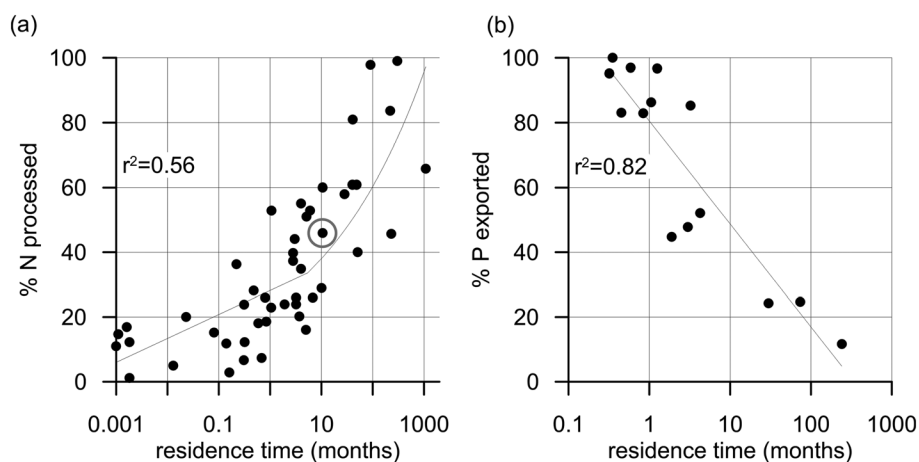


**Figure 5.** (a) Proportion of DIN processed in aquatic systems as a function of residence time [after S Seitzinger et al., 2006] (with permission from John Wiley & Sons). The circled point is a representative continental shelf identified in Seitzinger et al. [2006]. (b) Proportion of DIP exported from aquatic systems as a function of residence time [after Nixon et al., 1996] (with permission from Springer).

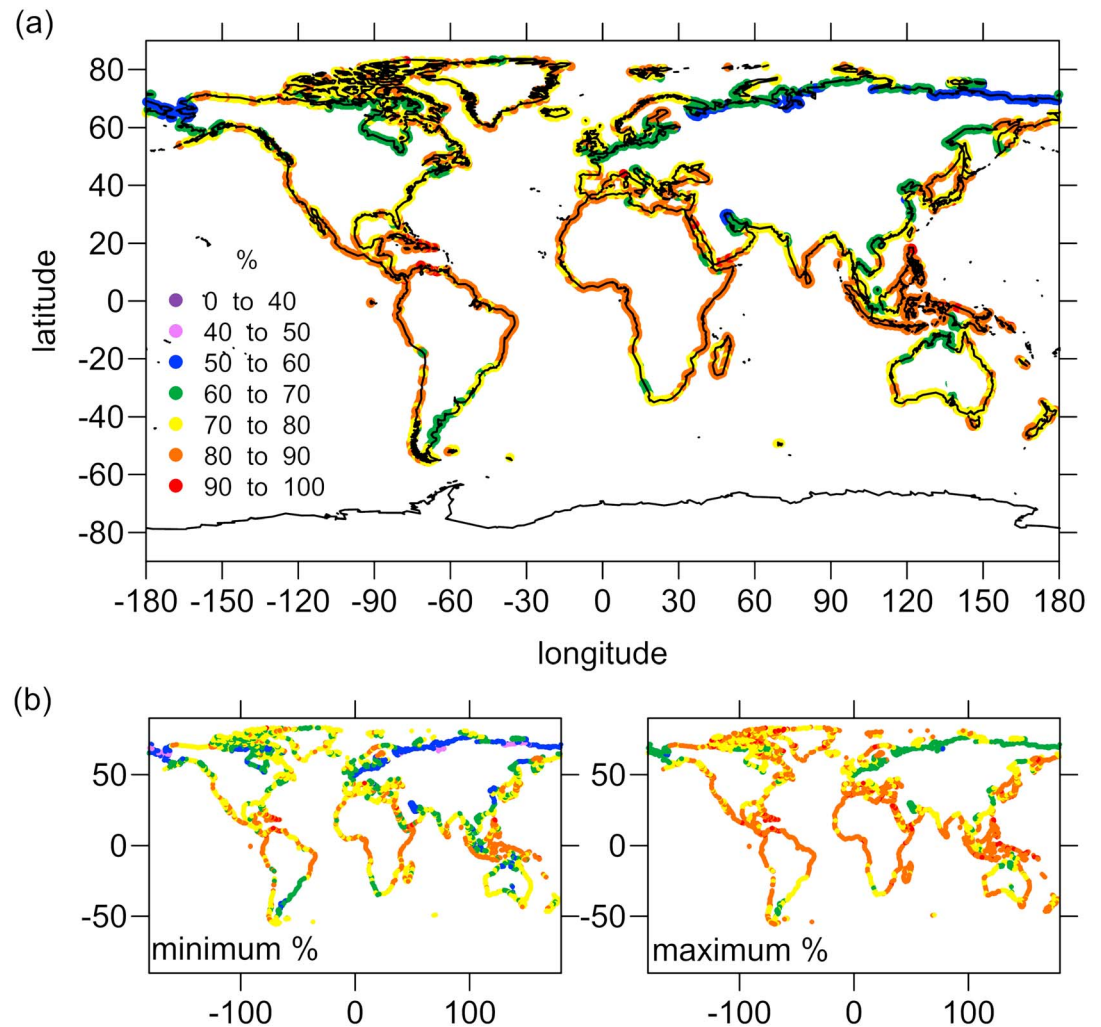


**Figure 6.** (a) Proportion of riverine DIN exported to the open ocean. (b) Uncertainties in export % based on uncertainties in  $T_{res}$  (Figure 4b).

### 3. Results

Using estimates of the relationships between inorganic nitrogen and phosphate export and residence time (Figure 5) [Nixon *et al.*, 1996; Seitzinger *et al.*, 2006] equations (11) and (12), combined with our own estimates of residence time on the shelf (Figure 4), we calculated the percentage of DIN and DIP from each riverine source that is exported from the shelf system into the open ocean (Figures 6 and 7). The plots of uncertainty ranges in the DIN (Figure 6b) and DIP delivery (Figure 7b) are based on the minimum and maximum values of  $T_{res}$  in Figure 4b. We acknowledge that there are additional substantial uncertainties in the relationships in Figure 5 and the exact relationship between removal and residence times requires further study. There are other more complex relationships to describe the rates of denitrification and its global range. For instance, the elegant study of Bohlen *et al.* [2012] requires estimates of sinking particulate organic carbon flux and bottom-water oxygen concentrations and as such is suitable for the global analysis of the magnitude of denitrification. It also implies a strong dependence on residence time. However, the data required to apply the Bohlen approach to shelf seas in the way we do here are not yet available. When it becomes available, it could be merged with the physical characterization included here to further improve estimates of shelf denitrification. A MATLAB function that calculates  $T_{res}$ ,  $S_p$ ,  $N_{export}$ , and  $P_{export}$  using our approach is available with this paper.

While the tropical and subtropical rivers tend to be most important for nutrient delivery, there are some significant proportions of riverine nutrients reaching the open ocean at temperate and high latitudes, for instance, off northwestern North America, southwestern South America, the Canadian Arctic, and Greenland. For the minimum of the

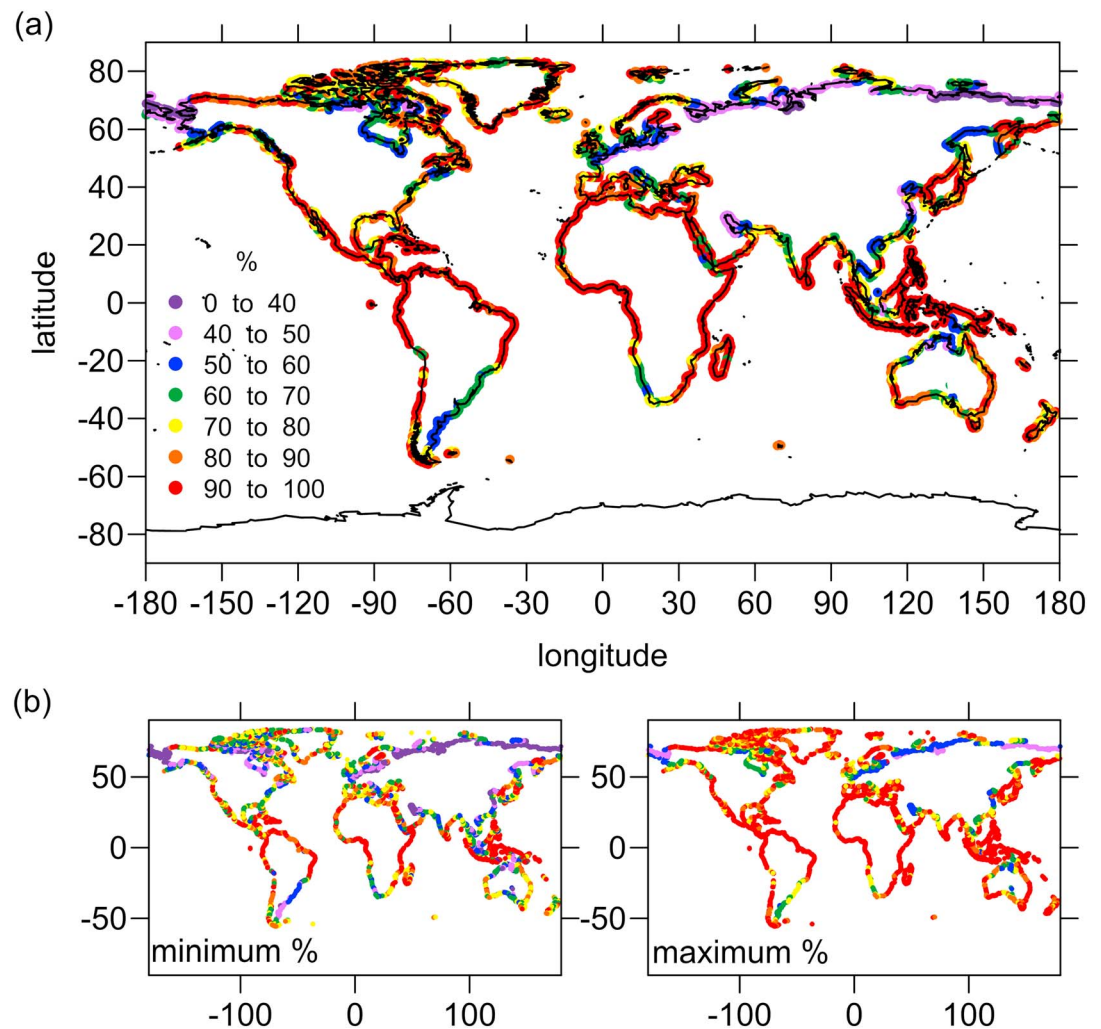


**Figure 7.** (a) Proportion of riverine DIP exported to the open ocean. (b) Uncertainties in export % based on uncertainties in  $T_{res}$  (Figure 4b).

uncertainty range (left panel in Figures 6b and 7b), where the analysis is based on conditions strongly limiting river plumes to the shelf with weak cross-plume and cross-shelf break transports, the region of high-nutrient delivery collapses onto the low latitudes. For the maximum of the uncertainty range (right panel in Figures 6b and 7b), with the widest river plumes and efficient cross-plume and cross-shelf break transports, nutrient delivery becomes almost uniformly high globally, with the Russian Arctic having the highest on-shelf processing of nutrients. Note that while we have assumed that processing of DIN is independent of latitude, in practice, denitrification and related anammox rates are dependent on temperature [Rysgaard *et al.*, 2004]. Our analysis suggests that nitrate retention will be more efficient at higher latitudes because of increased residence times associated with the Coriolis constraint on the width of the coastal buoyancy current. A decreasing rate of denitrification with cooler temperature at higher latitudes will act to offset this effect. Our range of residence times is greater than a factor of 50 (Figure 4), which results in a factor of about 2 change in nitrogen processing on the shelf (Figure 5a). The effect of a 10°C change in temperature on rates of anammox and denitrification is also a factor of 2 [Rysgaard *et al.*, 2004]. As anammox and denitrification are only part of the suite of processes affecting nitrogen, we would expect the latitudinal temperature range to have some effect on DIN processing but still leave a significant Coriolis-driven pattern. Also, the data used in the relationship in Figure 5 are taken from a range of systems between the subtropical and subpolar latitudes and so the effects of temperature are probably one of the sources of scatter in the relationship.

The global mean proportions of DIN and DIP that reach the ocean are 76% (minimum 72% and maximum 80%) and 79% (minimum 69% and maximum 85%), respectively. About half of the total range in the analysis

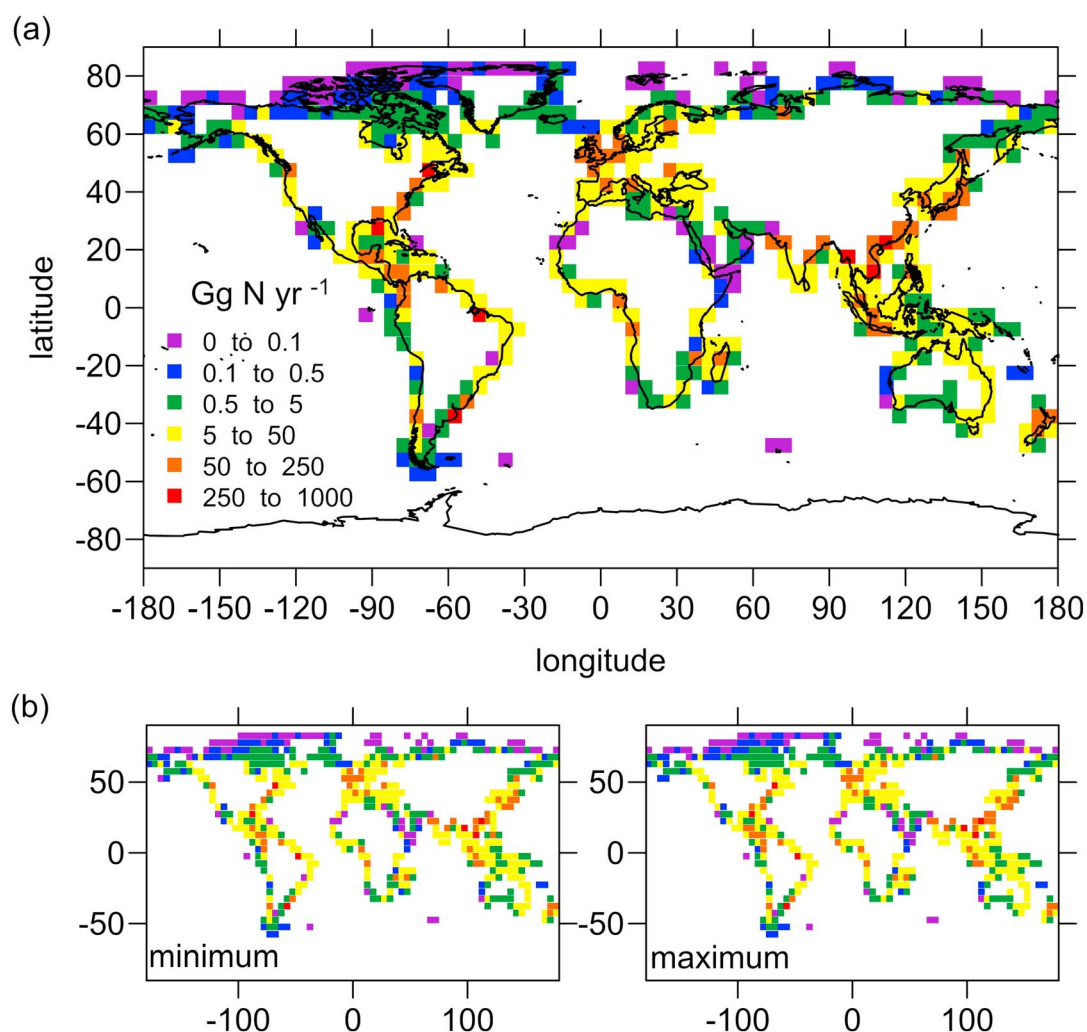


**Figure 8.** (a) DIN exported to the open ocean on a  $5^\circ \times 5^\circ$  global grid. (b) Uncertainties in DIN export based on uncertainties in  $T_{\text{res}}$  (Figure 4b). Note that these values do not take into account processing of riverine DIN within estuaries.

(Figures 6b and 7b) results from the range in the shelf-ocean exchange,  $E_{sb}$ . Considering the effect only of the 95% confidence intervals for  $c$  and  $a$ , both of the mean proportions of nutrient supply change only by  $\pm 1\%$ . The largest source of random error in the results lies with the regressions used to empirically link residence time to DIN and DIP processing, as described earlier.

If we ignore the processing of nutrients within estuaries and treat the nutrient loads in the NEWS 2 database [Mayorga *et al.*, 2010] as representing the upper bound of the amounts of DIN and DIP exiting estuaries onto the shelf, then we can estimate DIN and DIP supplies to the open ocean (Figures 8 and 9, with supplies calculated on a  $5^\circ \times 5^\circ$  global grid). The latitudinal pattern is still evident, driven now both by a tendency for large nutrient load rivers to be at lower latitudes and the latitudinal change in how efficiently plume water is exchanged with the open ocean, with the latter also influenced by the global pattern in shelf width. Major river sources at low latitudes are clear (e.g., the Amazon and rivers in Southeast Asia), but there are also significant sources at higher latitudes, notably the Mississippi (ranked fourth in N load globally) and the St. Lawrence (ranked tenth) in North America and the Parana in South America (ranked seventh).

#### 4. Discussion and Conclusions

Despite the difficulty in addressing riverine nutrient delivery from over 6000 rivers globally to the open ocean, we have made robust estimates of the proportion of DIN and DIP that could reach the open ocean.

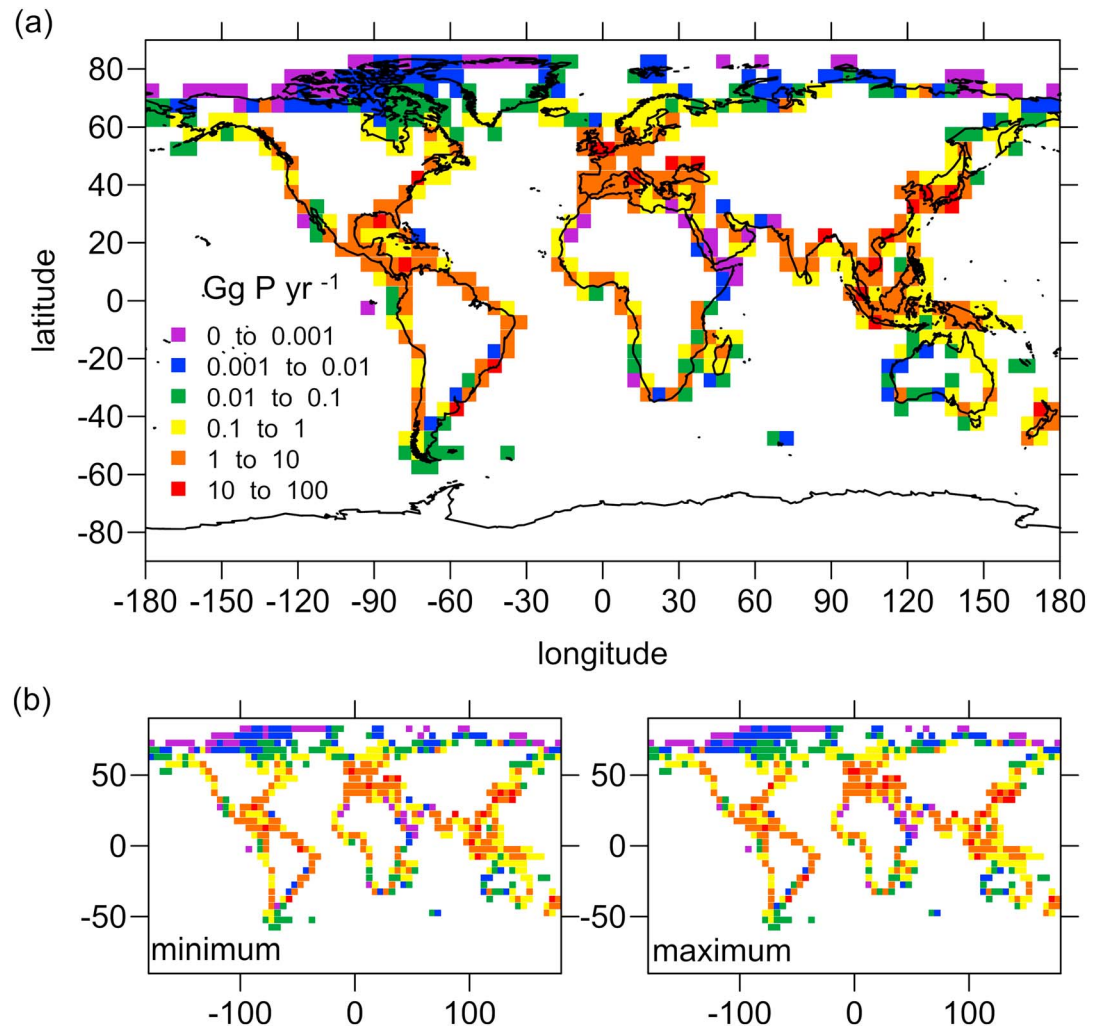


**Figure 9.** (a) DIP exported to the open ocean on a  $5^\circ \times 5^\circ$  global grid. (b) Uncertainties in DIP export based on uncertainties in  $T_{res}$  (Figure 4b). Note that these values do not take into account processing of riverine DIP within estuaries.

Our approach uses a scaling for the stratification and width of low-salinity buoyancy currents in coastal waters, providing global means with confidence intervals based on a sample of published studies on plumes. Comparing the buoyancy current width with the width of the local continental shelf determines whether within-plume transport processes or processes at the shelf break control the transfer of riverine material to the open ocean. Using estimates for these transport and exchange processes, along with their uncertainties, has allowed us to estimate residence times of riverine water on the continental shelves. These residence times were used with empirical relations to estimate the proportion of DIN and DIP that might leave the shelf and enter the open ocean. Finally, the global distribution of inputs of DIN and DIP to the open ocean was calculated, based on the proportions expected to be transferred across the shelf and the riverine DIN and DIP loads in the NEWS 2 database. Comparing the globally integrated riverine DIN and DIP deliveries with our calculations of the global amount of DIN and DIP reaching the ocean results in an average removal of 25% DIN and 19% DIP on the shelf, which will be augmented by estuarine retention. This suggests that significant quantities of riverine dissolved nutrients reach the open ocean. Of the 23 Tg DIN that are delivered to the land-ocean interface every year, 6 Tg are retained on the shelf and the other 17 Tg are delivered to the open ocean. Similarly, of the 1.6 Tg DIP delivered by rivers, 0.4 Tg are estimated to be retained on the shelf and 1.2 Tg reaches the open ocean. This DIP estimate could be an underestimate if there is extensive phosphorus release in estuaries [Froelich, 1988] although this is not universally true of all estuaries [Prastka et al., 1998].

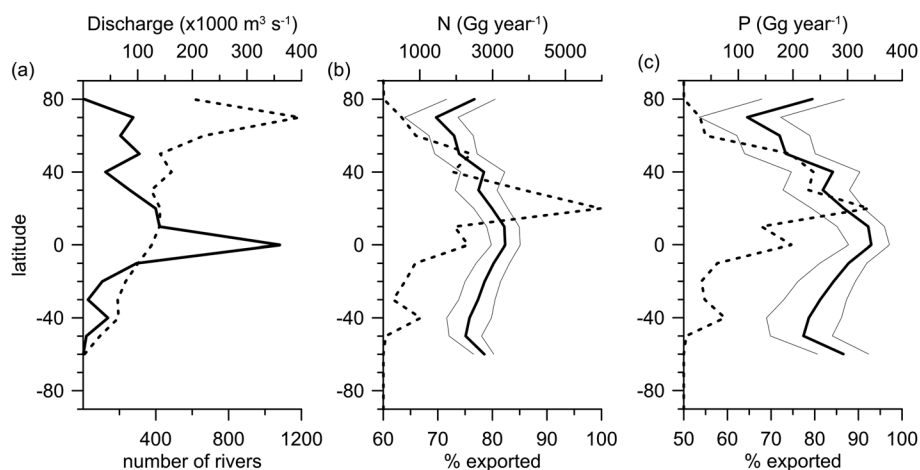


**Figure 10.** (a) Distribution of freshwater discharge (solid line) and the number of rivers (dashed line) within  $10^\circ$  latitude bands. (b) Riverine supply of DIN (dashed line) and percentage exported to the open ocean (solid line). (c) Riverine supply of DIP (dashed line) and percentage exported to the open ocean (solid line). In Figures 10b and 10c the bold solid line is the mean and thin solid lines show the uncertainties.

The latitudinal patterns and uncertainties are summarized by integrating the discharges and the proportions of nutrient reaching the open ocean in  $10^\circ$  latitudinal bands (Figure 10). The Amazon not surprisingly dominates the freshwater discharge, but it is also clear that freshwater supply to the shelf tends to be skewed to the Northern Hemisphere driven by the global distribution of land and by relatively small discharges from a large number of rivers (Figure 10a). DIN input is also skewed north as a result of higher loads in rivers draining more developed economic regions (e.g., NW Europe). There is a latitudinal effect on the export of DIN and DIP from the shelf system (Figures 10b and 10c), ranging between 70% and 80% for DIN and between 70% and 90% for DIP. The high proportion of exported DIN and DIP at low latitudes occurs in regions where the riverine supply of DIN and DIP is largest (Figures 10c and 10d), onto narrow shelves and where the width of buoyant plumes will be greater. The relatively short residence time of water over the shelf limits the scope for biogeochemical processing of the nutrients. This largely explains why our results are insensitive to variability in the internal Rossby radius and the ratio between plume width and internal Rossby radius. Even using conditions that constrain more plumes on the shelf, most of the major sources of DIN and DIP are at low latitudes and still have plumes that extend beyond the shelf break. The efficient delivery of nutrients to the open ocean by tropical rivers could magnify recent and anticipated increases in tropical nutrient loading on ocean productivity.

The uncertainties in the proportions of nutrients exported are typically  $\pm 5\%$  for DIN and  $\pm 5\text{--}10\%$  for DIP (Figures 10b and 10c). Given the assumptions and resulting uncertainties in  $T_{res}$  in our analyses, these uncertainties in exported nutrients perhaps appear small. This is so because changes in  $T_{res}$  need to be quite large in order to make a significant shift in the proportion of DIN or DIP reaching the ocean as calculated using the results of Figure 5; the range of residence times of plumes on the continental shelves is quite small compared to the total range of residence times in the aquatic systems used to generate Figure 5. The main sources of the uncertainties in Figure 10 are the wide range of cross-plume and cross-shelf break exchange rates used in the analyses. The other important source of uncertainty not included in Figure 10 arises from the equations fitted to the data in Figure 5, typically  $\pm 15\%$  in the proportions of DIN and DIP processed on the shelf.

It is perhaps surprising that our results suggest that high proportions of riverine DIN and DIP could reach the open ocean unmodified by shelf biogeochemistry, counter to the assumption that rivers are inefficient suppliers of nutrients beyond the shelf break [e.g., *Duce et al.*, 2008]. Assuming a high residence time for water on a continental shelf of almost 1 year (e.g., the circled point in Figure 5a) [*Seitzinger et al.*, 2006], then about 45% of DIN is processed on the shelf. Our analysis takes this further by suggesting that using such a shelf residence time as a global average would be incorrect (Figure 4a and Table 3), as continental shelves, particularly at low latitudes, can have much shorter residence times. While the more efficient nitrate removal at middle and high latitudes is consistent with the argument for effective processing of nitrogen in the shelf system [*Seitzinger et al.*, 2006], applying that argument globally will miss these key differences between low- and high-latitude systems associated with  $R'_o$  and shelf width.

**Table 4.** Distribution of Riverine DIN and DIP Supplies to the Major Ocean Basins<sup>a</sup>

Basin	Dissolved Inorganic N (Tg yr <sup>-1</sup> )			Dissolved Inorganic P (Tg yr <sup>-1</sup> )		
	Total	West	East	Total	West	East
North Atlantic Ocean	4.5	2.7	1.8	0.33	0.19	0.14
South Atlantic Ocean	1.8	1.5	0.3	0.18	0.17	0.01
North Pacific Ocean	4.5	4.1	0.4	0.28	0.26	0.03
South Pacific Ocean	0.9	0.7	0.2	0.10	0.08	0.02
Indian Ocean	4.4	0.8	3.6	0.27	0.05	0.23
Arctic	0.3			0.01		
Mediterranean	0.4			0.07		

<sup>a</sup>Note that these supplies do not account for processing in estuaries and so should be viewed as upper bounds.

Our global map of nutrient supply to the open ocean may be modified on seasonal time scales. In temperate regions, dissolved inorganic nutrients (nitrate, ammonium, phosphate, and silicate) are readily consumed by phytoplankton in the growing season (typical time scales of weeks to a few months) and upon settling the particulate detritus will be trapped at least temporarily in shelf sediments or bottom waters. Indeed, our analyses could be inverted to produce an estimate of riverine DIN and DIP available for primary production on the shelf, though noting that this would be a maximum estimate as some of the nutrient would be lost via other processes (e.g., denitrification and particle-water interactions). The phytoplankton uptake and settling removal mechanism only operates during the growing season; hence, seasonal variability in biogeochemical processing of nutrients on the shelf could lead to a seasonal modulation in the fluxes and relative proportions of nutrients reaching the open ocean in midlatitude and high-latitude systems. We also expect seasonality to reflect changes in freshwater flows and nutrient concentrations, particularly in Arctic and extratropical areas and those subject to monsoonal influence.

While we have focused on dissolved inorganic N and P, it is worth considering the implications of our results for dissolved organic carbon (DOC). Cycling of labile organic carbon in shelf systems is considerably faster than dissolved N and P. Labile dissolved organic matter is usually degraded with a half-life of about 10 days [Lonborg and Alvarez-Salgado, 2012], and rates are of the same order for labile riverine DOC in seawater [Rochelle-Newall et al., 2004]. Hence, outside of the tropical region, most labile DOC delivered to coastal waters by rivers and produced within them will be consumed on the shelf and not exported to the oceans; refractory DOC will be exported to the open ocean [Barrón and Duarte, 2015]. Low-latitude rivers are, however, relatively rich in dissolved organics and dominate riverine organic carbon delivery to the ocean [Ludwig et al., 1996]. The reduced Coriolis force near the equator means that labile DOC can reach the open ocean, as observed in the Amazon plume [Muller-Karger et al., 1988], and can contribute to the heterotrophic metabolic state of low-latitude ocean ecosystems [Duarte et al., 2013].

We have demonstrated that 75% of riverine DIN and 80% of DIP can reach the open ocean but that these supplies are variable depending on latitude, the width of the continental shelf, the riverine nutrient load, and the exchange of water across the shelf break. Compared to recent estimates of atmospheric deposition of nitrogen to the oceans [Jickells et al., submitted], the annual riverine supply of 17 Tg DIN is similar to the total annual deposition of oxidized N and is about 50% of the total atmospheric deposition of nitrogen. The annual riverine supply is about 10% of the supply via nitrogen fixation [Jickells et al., submitted]. Our results also indicate important basin-scale contrasts in riverine DIN and DIP supply (Table 4), with the western side of the Northern Hemisphere ocean basins tending to supply more DIN and DIP. These contrasts have implications for the importance of different nutrient supply routes to the oceans. Riverine N and P supplies tend to occur in different parts of the ocean compared to atmospheric N deposition or organic P delivery. For instance, relatively high riverine supplies of DIP in the western North Atlantic contrast with the importance of dissolved organic phosphorus in the east [Torres-Valdez et al., 2009]. Nitrogen fixation has a bias toward the eastern sides of the major ocean basins in the Northern Hemisphere [Jickells et al., submitted], while riverine DIN is biased to the west of the North Atlantic and North Pacific. Thus, the amounts of DIN and DIP delivered by rivers to the open ocean, combined with the spatial variability in the ability of shelf seas to process riverine nutrients, have the potential to alter global ocean productivity with a magnitude similar to other supply routes that are better quantified in global models. Thus, riverine nutrient supply needs to be incorporated into global models of nutrient cycling in order to yield more accurate results beyond assuming that either all or none of the riverine nutrient supply reaches the open ocean.

While our analysis has focused on dissolved inorganic N and P, the variable shelf retention time will have similar implications for the transport of other components such as trace metals with similar reactivity and sensitivity to residence times and for the issue of coastal eutrophication and “dead zones” [Diaz and Rosenberg, 2008]. Spatially resolved estimates of nutrient processing on shelves are needed for proper assessment of climate change-induced modification of the hydrological cycle and sea level. Low sea levels during the last glaciation had greatly reduced shelf width and potentially altered nutrient and carbon delivery to the open ocean. Current evidence suggests that the ocean nitrogen cycle changed considerably during the most recent postglacial warming [Galbraith *et al.*, 2013]. In the future, global warming is projected to lead to increased river discharge at high latitudes [Peterson *et al.*, 2002] and nutrient flows may well increase with an increasing human population [Seitzinger *et al.*, 2010]. The latitudinal variation of DIN and DIP export will need to be incorporated into models to allow realistic projections of the future behavior of both oceanic and coastal ecosystems.

### Acknowledgments

This paper resulted from the deliberations of GESAMP Working Group 38, the Atmospheric Input of Chemicals to the Ocean. We thank the ICSU Scientific Committee on Oceanic Research (SCOR), the U.S. National Science Foundation (NSF), the Global Atmosphere Watch (GAW) and the World Weather Research Programme (WWRP) of the World Meteorological Organization (WMO), the International Maritime Organization (IMO), and the University of East Anglia for support of this work. Additional support for J.S. came from the UK Natural Environment Research Council's Shelf Sea Biogeochemistry Research Programme (NE/K002007/1). J.M. was supported by the Netherlands Earth System Science Center (NESSC). K.F. was supported by the NSERC Discovery Program. We are indebted to two reviewers whose constructive feedback helped us to improve the paper. All data used in this paper can be found in the tables, figures, references, and in the supporting information.

### References

- Atkinson, L. P., A. Valle-Levinson, D. Figueroa, R. De Pol-Holz, V. A. Gallardo, W. Schneider, J. L. Blanco, and M. Schmidt (2002), Oceanographic observations in Chilean coastal waters between Valdivia and Concepcion, *J. Geophys. Res.*, *107*(C7), 3081, doi:10.1029/2001JC000991.
- Barrón, C., and C. M. Duarte (2015), Dissolved organic carbon pools and export from the coastal ocean, *Global Biogeochem. Cycles*, *29*, 1725–1738, doi:10.1002/2014GB005056.
- Bernard, C. Y., H. H. Durr, C. Heinze, J. Segsneider, and E. Maier-Reimer (2011), Contribution of riverine nutrients to the silicon biogeochemistry of the global ocean—A model study, *Biogeochemistry*, *8*(3), 551–564, doi:10.5194/bg-8-551-2011.
- Beusen, A. H. W., A. F. Bouwman, H. H. Durr, A. L. M. Dekkers, and J. Hartmann (2009), Global patterns of dissolved silica export to the coastal zone: Results from a spatially explicit global model, *Global Biogeochem. Cycles*, *23*, GB0A02, doi:10.1029/2008GB003281.
- Beusen, A. H. W., A. F. Bouwman, P. H. Van Beek, J. M. Mogollón, and J. J. Middelburg (2016), Global riverine N and P transport to ocean increased during the 20th century despite increased retention along the aquatic continuum, *Biogeochemistry*, *13*, 2441–2451, doi:10.5194/bg-13-2441-2016.
- Bohlen, L., A. W. Dale, and K. Wallmann (2012), Simple transfer functions for calculating benthic fixed nitrogen losses and C:N:P regeneration ratios in global biogeochemical models, *Global Biogeochem. Cycles*, *26*, GB3029, doi:10.1029/2011GB004198.
- Bourgeois, T., J. C. Orr, L. Resplandy, J. Terhaar, C. Ethe, M. Gehlen, and L. Bopp (2016), Coastal-ocean uptake of anthropogenic carbon, *Biogeochemistry*, *13*(14), 4167–4185.
- Breaker, L. C., and W. W. Broenkow (1994), The circulation of Monterey Bay and related processes, *Oceanogr. Mar. Biol.*, *32*(32), 1–64.
- Brink, K. H. (1998), Deep-sea forcing and exchange processes, in *The Sea, the Global Coastal Ocean: Processes and Methods*, edited by K. H. Brink and A. R. Robinson, pp. 151–167, John Wiley, New York.
- Carmack, E. C., and R. W. MacDonald (2002), Oceanography of the Canadian shelf of the Beaufort Sea: A setting for marine life, *Arctic*, *55*, 29–45.
- Choukroun, S., P. V. Ridd, R. Brinkman, and L. I. W. McKinna (2010), On the surface circulation in the western Coral Sea and residence times in the Great Barrier Reef, *J. Geophys. Res.*, *115*, C06013, doi:10.1029/2009JC005761.
- Condie, S. A. (2011), Modeling seasonal circulation, upwelling and tidal mixing in the Arafura and Timor Seas, *Cont. Shelf Res.*, *31*(14), 1427–1436, doi:10.1016/j.csr.2011.06.005.
- Denamiel, C., W. P. Budgell, and R. Toumi (2013), The Congo River plume: Impact of the forcing on the far-field and near-field dynamics, *J. Geophys. Res. Oceans*, *118*, 964–989, doi:10.1002/jgrc.20062.
- Diaz, R. J., and R. Rosenberg (2008), Spreading dead zones and consequences for marine ecosystems, *Science*, *321*, 926–928.
- Dong, L. X., J. L. Su, L. A. Wong, Z. Y. Cao, and J. C. Chen (2004), Seasonal variation and dynamics of the Pearl River plume, *Cont. Shelf Res.*, *24*(16), 1761–1777, doi:10.1016/j.csr.2004.06.006.
- Duarte, C. M., A. Regaudie-de-Gioux, J. M. Arrieta, A. Delgado-Huertas, and S. Agusti (2013), The oligotrophic ocean is heterotrophic, *Annu. Rev. Mar. Sci.*, *5*, 551–569, doi:10.1146/annurev-marine-121211-172337.
- Duce, R. A., et al. (2008), Impacts of atmospheric anthropogenic nitrogen on the open ocean, *Science*, *320*(5878), 893–897, doi:10.1126/science.1150369.
- Efron, B., and G. Gong (1983), A leisurely look at the bootstrap, the jackknife, and cross-validation, *Am. Stat.*, *37*(1), 36–48, doi:10.2307/2685844.
- Eicken, H., I. Dmitrenko, K. Tyshko, A. Darovskikh, W. Dierking, U. Blahak, J. Groves, and H. Kassens (2005), Zonation of the Laptev Sea landfast ice cover and its importance in a frozen estuary, *Global Planet. Change*, *48*(1–3), 55–83, doi:10.1016/j.gloplacha.2004.12.005.
- Estournel, C., P. Broche, P. Marsaleix, J. L. Devenon, F. Auclair, and R. Vehil (2001), The Rhone river plume in unsteady conditions: Numerical and experimental results, *Estuarine Coastal Shelf Sci.*, *53*(1), 25–38, doi:10.1006/ecss.2000.0685.
- Fennel, K., J. Wilkin, J. Levin, J. Moisan, J. O'Reilly, and D. Haidvogel (2006), Nitrogen cycling in the Middle Atlantic Bight: Results from a three-dimensional model and implications for the North Atlantic nitrogen budget, *Global Biogeochem. Cycles*, *20*, GB3007, doi:10.1029/2005GB002456.
- Fennel, K., et al. (2009), Modeling denitrification in aquatic sediments, *Biogeochemistry*, *93*(1–2), 159–178, doi:10.1007/s10533-008-9270-z.
- Fong, D. A., and W. R. Geyer (2002), The alongshore transport of freshwater in a surface-trapped river plume, *J. Phys. Oceanogr.*, *32*(3), 957–972, doi:10.1175/1520-0485(2002)032<0957:tatof>2.0.co;2.
- Frings, P. J., W. Clymans, G. Fontorbe, C. L. De La Rocha, and D. J. Conley (2016), The continental Si cycle and its impact on the ocean Si isotope budget, *Chem. Geol.*, *425*, 12–36.
- Froelich, P. N. (1988), Kinetic control of dissolved phosphate in natural rivers and estuaries—A primer on the phosphate buffer mechanism, *Limnol. Oceanogr.*, *33*(4), 649–668.
- Galbraith, E. D., et al. (2013), The acceleration of oceanic denitrification during deglacial warming, *Nat. Geosci.*, *6*, 579–584, doi:10.1038/ngeo1832.
- Garvine, R. W. (2001), The impact of model configuration in studies of buoyant coastal discharge, *J. Mar. Res.*, *59*(2), 193–225, doi:10.1357/002224001762882637.
- GEBCO (2008), General Bathymetric Chart of the Oceans, one minute grid version 2.

- Gelfenbaum, G., and R. P. Stumpf (1993), Observations of currents and density structure across a buoyant plume front, *Estuaries*, *16*(1), 40–52, doi:10.2307/1352762.
- Gersbach, G. H., C. B. Pattiaratchi, G. N. Ivey, and G. R. Cresswell (1999), Upwelling on the south-west coast of Australia—Source of the Capes Current?, *Cont. Shelf Res.*, *19*(3), 363–400, doi:10.1016/S0278-4343(98)00088-0.
- Geyer, W. R., R. C. Beardsley, S. J. Lentz, J. Candela, R. Limeburner, W. E. Johns, B. M. Castro, and I. D. Soares (1996), Physical oceanography of the Amazon shelf, *Cont. Shelf Res.*, *16*(5–6), 575–616, doi:10.1016/0278-4343(95)00051-8.
- Giraud, X., C. Le Quere, and L. C. da Cunha (2008), Importance of coastal nutrient supply for global ocean biogeochemistry, *Global Biogeochem. Cycles*, *22*, GB2025, doi:10.1029/2006GB002717.
- Gong, D., J. T. Kohut, and S. M. Glenn (2010), Seasonal climatology of wind-driven circulation on the New Jersey Shelf, *J. Geophys. Res.*, *115*, C04006, doi:10.1029/2009JC005520.
- Harrison, M. D., P. M. Groffman, P. M. Mayer, and S. S. Kaushal (2012), Microbial biomass and activity in geomorphic features in forested and urban restored and degraded streams, *Ecol. Eng.*, *38*, 1–10, doi:10.1016/j.ecoleng.2011.09.001.
- Hickey, B., S. Geier, N. Kachel, and A. F. MacFadyen (2005), A bi-directional river plume: The Columbia in summer, *Cont. Shelf Res.*, *25*(14), 1631–1656, doi:10.1016/j.csr.2005.04.010.
- Higgins, H. W., D. J. Mackey, and L. Clementson (2006), Phytoplankton distribution in the Bismarck Sea north of Papua New Guinea: The effect of the Sepik River outflow, *Deep-Sea Res. Part I*, *53*(11), 1845–1863, doi:10.1016/j.dsr.2006.09.001.
- Hordoir, R., K. D. Nguyen, and J. Polcher (2006), Simulating tropical river plumes, a set of parametrizations based on macroscale data: A test case in the Mekong Delta region, *J. Geophys. Res.*, *111*, C09036, doi:10.1029/2005JC003392.
- Horner-Devine, A. R., D. A. Jay, P. M. Orton, and E. Y. Spahn (2009), A conceptual model of the strongly tidal Columbia River plume, *J. Mar. Syst.*, *78*(3), 460–475, doi:10.1016/j.jmarsys.2008.11.025.
- Horner-Devine, A. R., R. D. Hetland, and D. G. MacDonald (2015), Mixing and transport in coastal river plumes, *Annu. Rev. Fluid Mech.*, *47*(47), 569–594, doi:10.1146/annurev-fluid-010313-141408.
- Houghton, R. W., R. J. Chant, A. Rice, and C. Tilburg (2009), Salt flux into coastal river plumes: Dye studies in the Delaware and Hudson River outflows, *J. Mar. Res.*, *67*(6), 731–756.
- Huthnance, J. M. (1995), Circulation, exchange and water masses at the ocean margin: The role of physical processes at the shelf edge, *Prog. Oceanogr.*, *35*(4), 353–431, doi:10.1016/0079-6611(95)00012-6.
- Huthnance, J. M. (1997), North Sea interaction with the North Atlantic Ocean, *Dtsch. Hydrogr. Z.*, *49*, 153–162.
- Huthnance, J. M. (2010), The Northeast Atlantic margins, in *Carbon and Nutrient Fluxes in Continental Margins: A Global Synthesis*, edited by K.-K. Liu et al., pp. 215–234, Springer, Berlin.
- Huthnance, J. M., H. M. Van Aken, M. White, E. D. Barton, B. Le Cann, E. F. Coelho, E. A. Fanjul, P. Miller, and J. Vitorino (2002), Ocean margin exchange—Water flux estimates, *J. Mar. Syst.*, *32*(1–3), 107–137, doi:10.1016/S0924-7963(02)00034-9.
- Huthnance, J. M., J. T. Holt, and S. L. Wakelin (2009), Deep ocean exchange with west-European shelf seas, *Ocean Sci.*, *5*(4), 621–634, doi:10.5194/os-5-621-2009.
- Jickells, T. D., and K. Weston (2011), Nitrogen cycle—external cycling: Losses and gains, in *Treatise on Estuarine and Coastal Science*, edited by E. Wolanski and D. S. McLusky, pp. 261–278, Elsevier, Amsterdam.
- Jickells, T. D., et al. (submitted), A re-evaluation of the magnitude and impacts of anthropogenic atmospheric nitrogen inputs on the ocean, *Global Biogeochem. Cycles*.
- Josey, S. A., E. C. Kent, and P. K. Taylor (2002), Wind stress forcing of the ocean in the SOC climatology: Comparisons with the NCEP-NCAR, ECMWF, UWM/COADS, and Hellerman and Rosenstein Datasets, *J. Phys. Oceanogr.*, *32*(7), 1993–2019, doi:10.1175/1520-0485(2002)032<1993:wsfoto>2.0.co;2.
- Knudsen, M. (1900), Ein hydrographischer Lehrsatz, *Ann. Hydrogr. Mar. Meteorol.*, *28*, 316–320.
- Laruelle, G. G., et al. (2009), Anthropogenic perturbations of the silicon cycle at the global scale: Key role of the land-ocean transition, *Global Biogeochem. Cycles*, *23*, GB4031, doi:10.1029/2008GB003267.
- Liste, M., M. Grifoll, and J. Monbaliu (2014), River plume dispersion in response to flash flood events. Application to the Catalan shelf, *Cont. Shelf Res.*, *87*, 96–108, doi:10.1016/j.csr.2014.06.007.
- Liu, J. T., S. Y. Chao, and R. T. Hsu (1999), The influence of suspended sediments on the plume of a small mountainous river, *J. Coast. Res.*, *15*(4), 1002–1010.
- Lonborg, C., and X. A. Alvarez-Salgado (2012), Recycling versus export of bioavailable dissolved organic matter in the coastal ocean and efficiency of the continental shelf pump, *Global Biogeochem. Cycles*, *26*, GB3018, doi:10.1029/2012GB004353.
- Ludwig, W., P. AmiotteSuchet, and J. L. Probst (1996), River discharges of carbon to the world's oceans: Determining local inputs of alkalinity and of dissolved and particulate organic carbon, *C. R. Acad. Sci. Ser. II Fascicule Sci. La Terre Et Des Planetes*, *323*(12), 1007–1014.
- Maavara, T., C. T. Parsons, C. Ridenour, S. Stojanovic, H. H. Dürr, H. R. Powley, and P. Van Cappellen (2015), Global phosphorus retention by river damming, *Proc. Natl. Acad. Sci. U.S.A.*, *112*, 15,603–15,608, doi:10.1073/pnas.1511797112.
- MacKenzie, F. T., L. M. Ver, and A. Lerman (2000), Coastal-zone biogeochemical dynamics under global warming, *Int. Geol. Rev.*, *42*(3), 193–206.
- Mayorga, E., S. P. Seitzinger, J. A. Harrison, E. Dumont, A. H. W. Beusen, A. F. Bouwman, B. M. Fekete, C. Kroeze, and G. Van Drecht (2010), Global Nutrient Export from WaterSheds 2 (NEWS 2): Model development and implementation, *Environ. Modell. Software*, *25*(7), 837–853, doi:10.1016/j.envsoft.2010.01.007.
- Middelburg, J. J., and K. Soetaert (2004), The role of sediments in shelf ecosystem dynamics, *Geochim. Et Cosmochim. Acta*, *68*(11), A343–A343.
- Moebius, J., and K. Daehnke (2015), Nitrate drawdown and its unexpected isotope effect in the Danube estuarine transition zone, *Limnol. Oceanogr.*, *60*(3), 1008–1019, doi:10.1002/lno.10068.
- Moore, J. K., and S. C. Doney (2007), Iron availability limits the ocean nitrogen inventory stabilizing feedbacks between marine denitrification and nitrogen fixation, *Global Biogeochem. Cycles*, *21*, GB2001, doi:10.1029/2006GB002762.
- Moore, W. S. (2007), Seasonal distribution and flux of radium isotopes on the southeastern US continental shelf, *J. Geophys. Res.*, *112*, C10013, doi:10.1029/2007JC004199.
- Moore, W. S., and J. de Oliveira (2008), Determination of residence time and mixing processes of the Ubatuba, Brazil, inner shelf waters using natural Ra isotopes, *Estuarine Coastal Shelf Sci.*, *76*(3), 512–521, doi:10.1016/j.ecss.2007.07.042.
- Muller-Karger, F. E., C. R. McClain, and P. L. Richardson (1988), The dispersal of the Amazon's water, *Nature*, *333*(6168), 56–59, doi:10.1038/333056a0.
- Mulligan, R. P., W. Perrie, and S. Solomon (2010), Dynamics of the Mackenzie River plume on the inner Beaufort shelf during an open water period in summer, *Estuarine Coastal Shelf Sci.*, *89*(3), 214–220, doi:10.1016/j.ecss.2010.06.010.
- Munchow, A., and R. W. Garvine (1993), Buoyancy and wind forcing of a coastal current, *J. Mar. Res.*, *51*(2), 293–322, doi:10.1357/0022240933223747.

- Narayanan, C., and R. W. Garvine (2002), Large scale buoyancy driven circulation on the continental shelf, *Dynam. Atmos. Oceans*, 36(1–3), 125–152.
- Nehama, F. P. J., and C. J. C. Reason (2014), Morphology of the Zambezi River Plume on the Sofala Bank, Mozambique, *Western Indian Ocean J. Mar. Sci.*, 13(1), 1–10.
- Nixon, S. W., J. Ammerman, and L. Atkinson (1996), The fate of nitrogen and phosphorus at the land sea margin of the North Atlantic Ocean, *Biogeochemistry*, 35(1), 141–180, doi:10.1007/BF02179826.
- Nof, D., and T. Pichevin (2001), The ballooning of outflows, *J. Phys. Oceanogr.*, 31(10), 3045–3058, doi:10.1175/1520-0485(2001)031<3045:tboo>2.0.co;2.
- Peterson, B. J., R. M. Holmes, J. W. McClelland, C. J. Vorosmarty, R. B. Lammers, A. I. Shiklomanov, I. A. Shiklomanov, and S. Rahmstorf (2002), Increasing river discharge to the Arctic Ocean, *Science*, 298(5601), 2171–2173, doi:10.1126/science.1077445.
- Polton, J. A., M. R. Palmer, and M. J. Howarth (2011), Physical and dynamical oceanography of Liverpool Bay, *Ocean Dynam.*, 61(9), 1421–1439, doi:10.1007/s10236-011-0431-6.
- Prastka, K., R. Sanders, and T. Jickells (1998), Has the role of estuaries as sources or sinks of dissolved inorganic phosphorus changed over time? Results of a Kd study, *Mar. Pollut. Bull.*, 36, 718–728.
- Rabalais, N. N., R. E. Turner, and W. J. Wiseman (2002), Gulf of Mexico hypoxia, aka “the dead zone”, *Annu. Rev. Ecol. Syst.*, 33, 235–263, doi:10.1146/annurev.ecolsys.33.010802.150513.
- Rabouille, C., F. T. Mackenzie, and L. M. Ver (2001), Influence of the human perturbation on carbon, nitrogen, and oxygen biogeochemical cycles in the global coastal ocean, *Geochim. Cosmochim. Acta*, 65(21), 3615–3641, doi:10.1016/s0016-7037(01)00760-8.
- Regnier, P., et al. (2013), Anthropogenic perturbation of the carbon fluxes from land to ocean, *Nat. Geosci.*, 6(8), 597–607.
- Ren, J. L., J. Zhang, J. B. Li, X. Y. Yu, S. M. Liu, and E. R. Zhang (2006), Dissolved aluminum in the Yellow Sea and East China Sea—Al as a tracer of Changjiang (Yangtze River) discharge and Kuroshio incursion, *Estuarine Coastal Shelf Sci.*, 68(1–2), 165–174, doi:10.1016/j.ecss.2006.02.004.
- Rennie, S. E., J. L. Largier, and S. J. Lentz (1999), Observations of a pulsed buoyancy current downstream of Chesapeake Bay, *J. Geophys. Res.*, 104(C8), 18,227–18,240, doi:10.1029/1999JC900153.
- Rochelle-Newall, E. J., M. D. Pizay, J. J. Middelburg, H. T. S. Boschker, and J. P. Gattuso (2004), Degradation of riverine dissolved organic matter by seawater bacteria, *Aquat. Microb. Ecol.*, 37(1), 9–22, doi:10.3354/ame037009.
- Rysgaard, S., R. N. Glud, N. Risgaard-Petersen, and T. Dalsgaard (2004), Denitrification and anammox activity in Arctic marine sediments, *Limnol. Oceanogr.*, 49(5), 1493–1502.
- Sanders, T. M., and R. W. Garvine (2001), Fresh water delivery to the continental shelf and subsequent mixing: An observational study, *J. Geophys. Res.*, 106(C11), 27,087–27,101, doi:10.1029/2001JC000802.
- Schiller, R. V., V. H. Kourafalou, P. Hogan, and N. D. Walker (2011), The dynamics of the Mississippi River plume: Impact of topography, wind and offshore forcing on the fate of plume waters, *J. Geophys. Res.*, 116, C06029, doi:10.1029/2010JC006883.
- Seitzinger, S. P., J. A. Harrison, E. Dumont, A. H. W. Beusen, and A. F. Bouwman (2005), Sources and delivery of carbon, nitrogen, and phosphorus to the coastal zone: An overview of Global Nutrient Export from Watersheds (NEWS) models and their application, *Global Biogeochem. Cycles*, 19, GB4S01, doi:10.1029/2005GB002606.
- Seitzinger, S. P., et al. (2010), Global river nutrient export: A scenario analysis of past and future trends, *Global Biogeochem. Cycles*, 24, GB0A08, doi:10.1029/2009GB003587.
- Seitzinger, S., J. A. Harrison, J. K. Bohlke, A. F. Bouwman, R. Lowrance, B. Peterson, C. Tobias, and G. Van Drecht (2006), Denitrification across landscapes and waterscapes: A synthesis, *Ecol. Appl.*, 16(6), 2064–2090, doi:10.1890/1051-0761(2006)016[2064:dalawa]2.0.co;2.
- Sharples, J., and J. H. Simpson (1993), Periodic frontogenesis in a region of freshwater influence, *Estuaries*, 16(1), 74–82, doi:10.2307/1352765.
- Simpson, J. H., W. G. Bos, F. Schirmer, A. J. Souza, T. P. Rippeth, S. E. Jones, and D. Hydes (1993), Periodic stratification in the Rhine ROFI in the North Sea, *Oceanol. Acta*, 16(1), 23–32.
- Souza, A. J., J. H. Simpson, and F. Schirmer (1997), Current structure in the Rhine region of freshwater influence, *J. Mar. Res.*, 55(2), 277–292, doi:10.1357/0022240973224409.
- Statham, P. J. (2012), Nutrients in estuaries—An overview and the potential impacts of climate change, *Sci. Total Environ.*, 434, 213–227, doi:10.1016/j.scitotenv.2011.09.088.
- Torres-Valdez, S., V. M. Roussenov, R. Sanders, S. Reynolds, X. Pan, R. Mather, A. Landolfi, G. A. Wolff, E. P. Achterberg, and R. G. Williams (2009), Distribution of dissolved organic nutrients and their effect on export production over the Atlantic Ocean, *Global Biogeochem. Cycles*, 23, GB4019, doi:10.1029/2008GB003389.
- Treguer, P., D. M. Nelson, A. J. Vanbennekorn, D. J. Demaster, A. Leynaert, and B. Queguiner (1995), The silica balance in the world ocean—A reestimate, *Science*, 268(5209), 375–379, doi:10.1126/science.268.5209.375.
- Weingartner, T. J., S. L. Danielson, and T. C. Royer (2005), Freshwater variability and predictability in the Alaska Coastal Current, *Deep Sea Res. Part II*, 52(1–2), 169–191, doi:10.1016/j.dsr2.2004.09.030.
- Whitney, M. M., and R. W. Garvine (2006), Simulating the Delaware Bay buoyant outflow: Comparison with observations, *J. Phys. Oceanogr.*, 36(1), 3–21, doi:10.1175/jpo2805.1.
- Yankovsky, A. E., and D. C. Chapman (1997), A simple theory for the fate of buoyant coastal discharges, *J. Phys. Oceanogr.*, 27(7), 1386–1401, doi:10.1175/1520-0485(1997)027<1386:astftf>2.0.co;2.
- Zatsepin, A. G., P. O. Zavialov, V. V. Kremenskiy, S. G. Poyarkov, and D. M. Soloviev (2010), The upper desalinated layer of the Kara Sea, *Oceanology*, 50(5), 657–667.